Differences of Convex Functions in Robust Data-Driven MPC: Part II

Mark Cannon, Yana Lishkova

Department of Engineering Science
University of Oxford, UK

mark.cannon@eng.ox.ac.uk

Motivation

Real applications (aerospace, automotive, biomedical, process control...) involve

- nonlinear dynamics
- unknown disturbance inputs and uncertain model parameters
- constraints on states and control inputs

... and typically need

- reliable, scalable, convex problem formulations
- robust control strategies allowing online parameter learning

Outline

1. Recap: difference of convex (DC) tube (T)MPC via convex-concave procedure
2. Constructing DC models using polynomial approximations and ICNNs
3. Tube geometry is important!
4. Robustness to disturbances and recursive feasibility
5. Application examples:
    - tiltwing VTOL transition with wind-gust uncertainty
    - robust adaptive control of batch-fed bioreactor
    - data-driven control for closed loop deep brain stimulation

Recap: MPC nonlinear program

Nominal case (no disturbances)

$$
\begin{aligned}
\mathcal{P}_t : \quad \underset{\{u_k\},\{x_k\}}{\text{minimize}} \quad & l_{\mathbb{T}}(x_N) + \sum_{k=0}^{N-1} l_k(x_k, u_k) \\
\text{s.t.} \quad & x_0 = x_t^p \\
& x_N \in \mathcal{X}_{\mathbb{T}} \\
& x_{k+1} = f(x_k, u_k) \\
& x_k \in \mathcal{X} \\
& u_k \in \mathcal{U} \\
& \text{for } k = 0, \ldots, N-1
\end{aligned}
$$

- MPC law: $u_t^p = u_0^*$ at time t, where $\{u_0^*, \ldots, u_{N-1}^*\}$ solves $\mathcal{P}_t$
- $l_k(\cdot,\cdot)$, $\mathcal{X}$, $\mathcal{U}$ convex; terminal cost $l_{\mathbb{T}}(\cdot)$ & terminal set $\mathcal{X}_{\mathbb{T}}$ convex

Recap: DC-TMPC convex program

$$
\begin{aligned}
\hat{\mathcal{P}}_t : \underset{\mathbf{v},\mathbf{X}}{\text{minimize}} \quad & \max_{x \in \mathcal{X}_N} l_{\mathbb{T}}(x) + \sum_{k=0}^{N-1} \max_{x \in \mathcal{X}_k} l_k(x, Kx + v_k) \\
\text{s.t.} \quad & x_t^p \in \mathcal{X}_0 \\
& \mathcal{X}_N \subseteq \mathcal{X}_{\mathbb{T}} \\
& \hat{f}_Q(x, Kx + v_k) \leq q_{k+1} \ \forall x \in \mathcal{V}(\mathcal{X}_k) \\
& \mathcal{X}_k \subseteq \mathcal{X} \\
& K\mathcal{X}_k + v_k \subseteq \mathcal{U} \\
& \text{for } k = 0, \dots, N-1
\end{aligned}
$$

- Solution $\mathbf{v}^* = \{v_0^*, \dots, v_{N-1}^*\}$, $\mathbf{X}^* = \{\mathcal{X}_0^*, \dots, \mathcal{X}_N^*\}$
- Vertices $\mathcal{V}(\mathcal{X}_k)$, $k = 0, \dots, N$ used in objective and constraints

Recap: DC-TMPC sequential convex program

Input: Seed trajectory $(\mathbf{x}^\circ, \mathbf{u}^\circ)$ satisfying: $x_0^\circ = x_t^p$, $x_N^\circ \in \mathcal{X}_\mathbb{T}$, and
$(x_k^\circ, u_k^\circ) \in \mathcal{X} \times \mathcal{U}$, $x_{k+1}^\circ = f(x_k^\circ, u_k^\circ)$, $k = 0, \dots, N-1$

Iteration: set $i \leftarrow 0$ $J_t^{(-1)} \leftarrow \infty$, $\mathit{flag} \leftarrow 1$

while flag

solve $\hat{\mathcal{P}}_t$ and set $J_t^{(i)} \leftarrow \mathrm{value}(\hat{\mathcal{P}}_t)$
$(\mathbf{v}^{(i)}, \mathbf{X}^{(i)}) \leftarrow (\mathbf{v}^*, \mathbf{X}^*)$
$i \leftarrow i + 1$

update $(\mathbf{x}^\circ, \mathbf{u}^\circ)$: $u_k^\circ \leftarrow K x_k^\circ + v_k^*$
$x_{k+1}^\circ \leftarrow f(x_k^\circ, u_k^\circ)$, $k = 0, \dots N-1$

if $i \geq \mathit{maxiters}$ or $J_t^{(i-2)} - J_t^{(i-1)} < \mathit{tolerance}$
set $\mathit{flag} \leftarrow 0$

Output: $\{u_0^*, \dots, u_{N-1}^*\}$, $\{x_0^*, \dots, x_N^*\}$, $\mathrm{value}(\hat{P}_t)$

Recap: DC-TMPC properties

- At any given time t:
  - $\hat{\mathcal{P}}_t$ is feasible at each iteration $i = 0, 1 \ldots$
  - $J_t^{(i)} \rightarrow J_{\text{NLP}}^*$ as $i \rightarrow \infty$
  - $\mathbf{X}^{(i)} \rightarrow \mathbf{x}_{\text{NLP}}^*$ as $i \rightarrow \infty$

  where J_{NLP}^* and $\mathbf{x}_{\text{NLP}}^*$ are an optimal cost value and state trajectory for $\mathcal{P}_t$

Recap: DC-TMPC properties

- At any given time t:
  - $\hat{\mathcal{P}}_t$ is feasible at each iteration $i = 0, 1 \dots$
  - $J_t^{(i)} \to J_{\mathrm{NLP}}^*$ as $i \to \infty$
  - $\mathbf{X}^{(i)} \to \mathbf{x}_{\mathrm{NLP}}^*$ as $i \to \infty$

  where J_{NLP}^* and $\mathbf{x}_{\mathrm{NLP}}^*$ are an optimal cost value and state trajectory for $\mathcal{P}_t$

- For any $maxiters \geq 1$, if $(\mathbf{x}^\circ, \mathbf{u}^\circ)$ at time t is computed using the solution of the final iteration at $t-1$, then the MPC law $u_t = u_0^*$ for all t ensures that:
  - $\hat{\mathcal{P}}_t$ is recursively feasible
  - $J_t^{(i)}$ is monotonically non-increasing in both i and t

Outline

1. Recap: difference of convex (DC) tube (T)MPC via convex-concave procedure
2. Constructing DC models using polynomial approximations and ICNNs
3. Tube geometry is important!
4. Robustness to disturbances and recursive feasibility
5. Application examples:
   - tiltwing VTOL transition with wind-gust uncertainty
   - robust adaptive control of batch-fed bioreactor
   - data-driven control for closed loop deep brain stimulation

DC decomposition via polynomial approximation

1. Generate samples $f(x^{(i)})$, $i = 1, \ldots, N_s$ and fit a polynomial $f(x) \approx y^\top F y$ e.g. by least squares:

$$\underset{F}{\text{minimize}} \sum_{i=1}^{N_s} \|f(x^{(i)}) - y(x^{(i)})^\top F y(x^{(i)})\|_2^2$$

   where $y(x) = [1, x_1, \ldots, x_n, x_1 x_2, \ldots, x_n^d]^\top$ is a vector of monomials

2. Find G, H so that $y^\top F y = y^\top G y - y^\top H y$, with $y^\top G y$, $y^\top H y$ convex in x e.g. by SDP:

$$\underset{G,H}{\text{maximize}} \;\; \sigma \;\; \text{s.t.} \;\; \mathbf{H}(G) \succeq \sigma I, \;\; \mathbf{H}(G - F) \succeq \sigma I$$

DC decomposition via polynomial approximation

Example: $f(x) = \exp\{-2(x_2 - 0.4)^2 - 2x_1^2\}$
$N_s = 50$ samples, $d = 4$, $H, G \in \mathbb{R}^{15\times 15}$

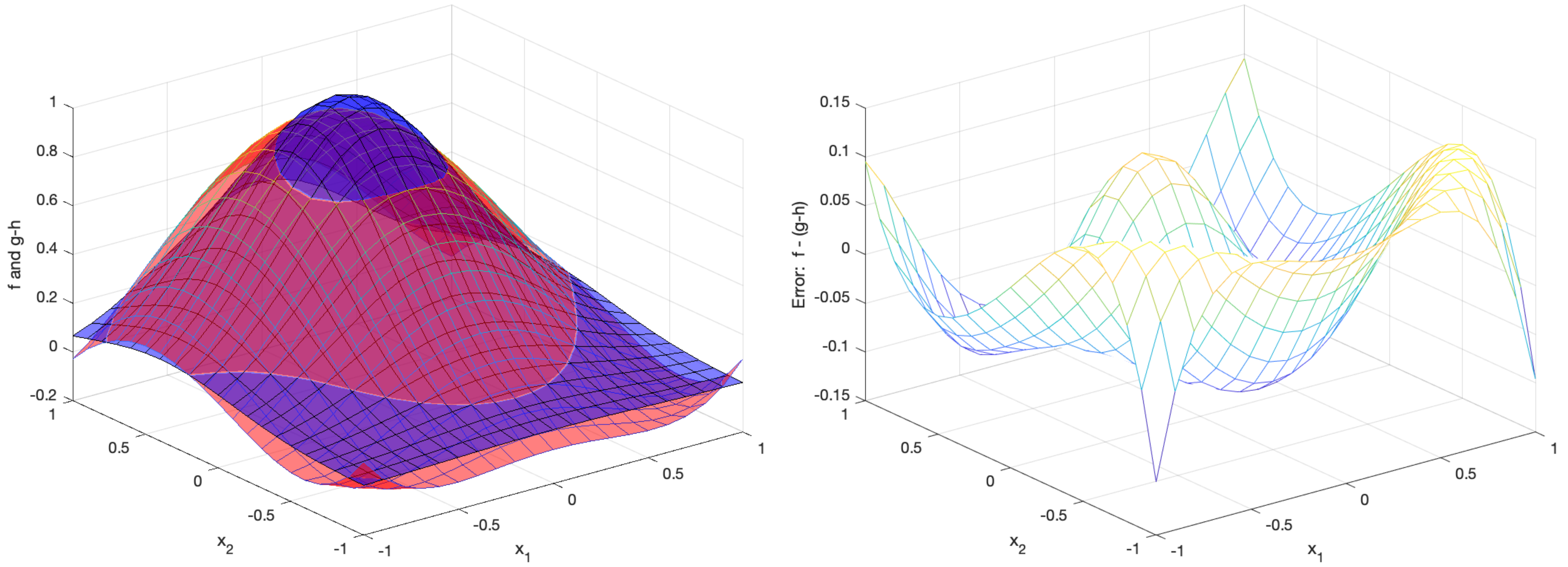

DC decomposition via feedforward or recurrent neural networks

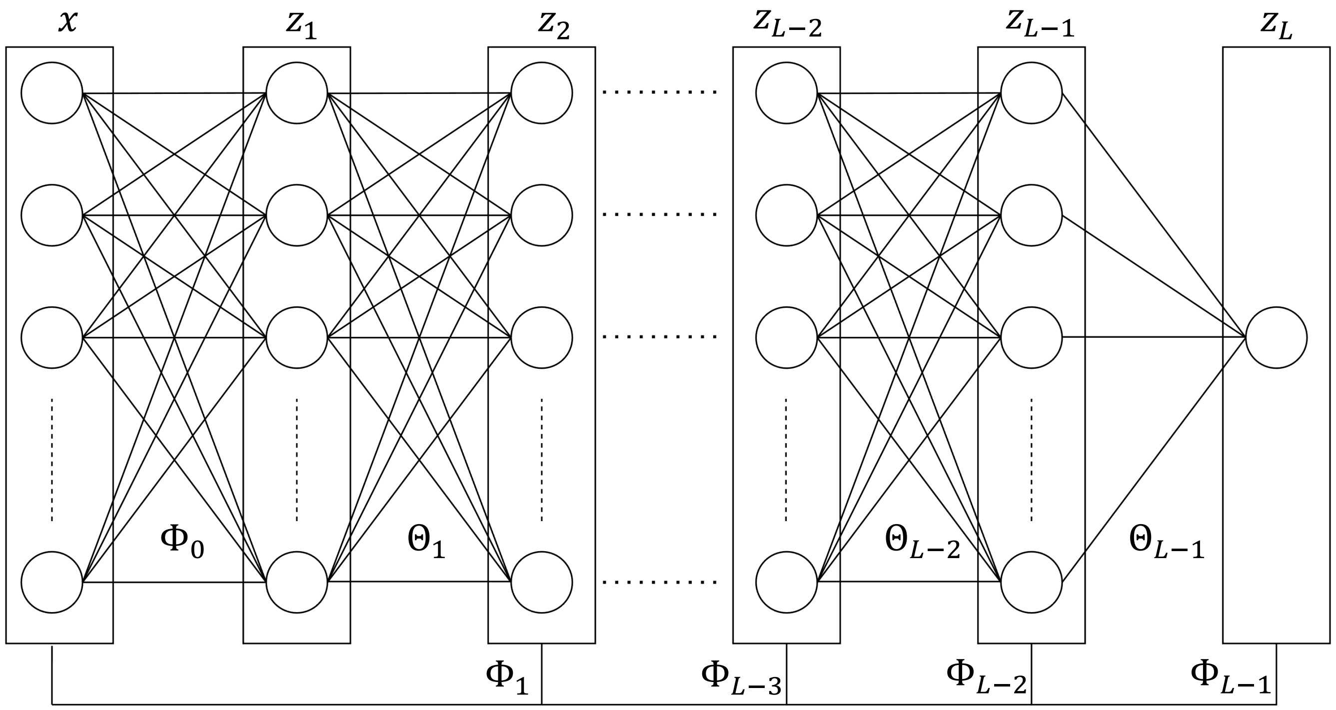

- Input-output map $z_L = f(x;\theta)$
  parameters: $\theta = \{\Theta_l, \Phi_l, b_l\}$

- $f(x,\theta)$ is componentwise convex in x if:
  - kernel weights are non-negative: $\Theta_l \geq 0 \; \forall l$
  - activation functions $\sigma(\cdot)$ are convex and non-decreasing

- $z_{l+1} = \sigma(\Theta_l z_l + \Phi_l x + b_l)$, for $l = 0, \ldots, L-1$
  ReLU activation function: $\sigma(x) = \max\{0, x\}$

DC decomposition using DC feedforward NNs

- $f(x;\theta)$ is DC (i.e. a DCNN) if $\Theta_l \geq 0\ \forall l < L-1$ and Θ_{L-1} is unconstrained
- DCNNs have advantages over DC polynomial approximations in DC-TMPC:
  - easier training (no need for LMIs and large-scale SDPs)
  - faster evaluation

$$f(x,\theta) = (\sigma \circ \mathcal{A}_{\theta_{L-1},x} \circ \cdots \circ \sigma \circ \mathcal{A}_{\theta_1,x} \circ \sigma \circ \mathcal{A}_{\Phi_0})(x)$$

    where $\mathcal{A}_{\theta_l,x}(z) = \Theta_l z + \Phi_l x + b_l$, and $\mathcal{A}_{\Phi_0}(x) = \Phi_0 x + b_0$

  - faster linearization; e.g. if $\sigma = \max\{0,x\}$ and $H(x) = \mathbf{1}_{x\geq 0}$, then

$$\frac{\partial f}{\partial x} = (H \circ \Theta_{L-1} \circ \cdots \circ H \circ \Theta_1 \circ \Phi_0)(x)$$

Example: Quadcopter control

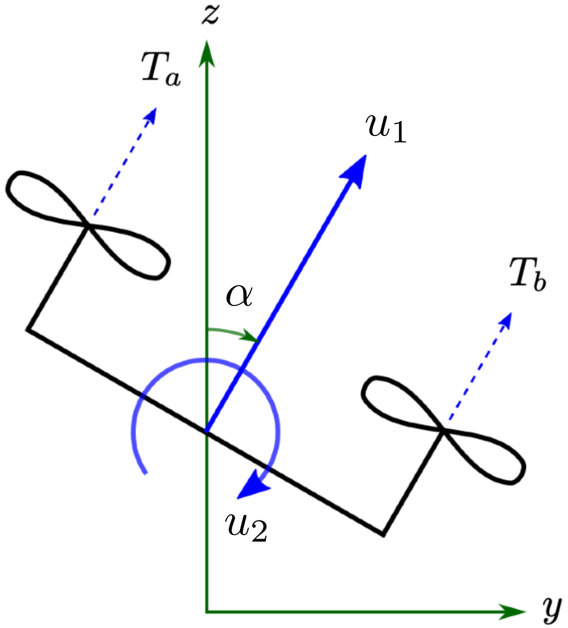

Model state $x = (y, z, \alpha, \dot{y}, \dot{z}, \dot{\alpha})$,

$$\ddot{y} = (u_1 + g)\sin\alpha, \;\; \ddot{z} = (u_1 + g)\cos\alpha - g, \;\; \ddot{\alpha} = u_2$$

y, z, α:	horizontal, vertical and angular displacement
u_1, u_2:	control inputs proportional to net thrust and torque

Constraints: $|u_1| \leq 10, |u_2| \leq 10, \; |\alpha| \leq 3, \; |\dot{\alpha}| \leq 1, \; |\dot{y}| \leq 30, \; |\dot{z}| \leq 10$

Example: Quadcopter modelling

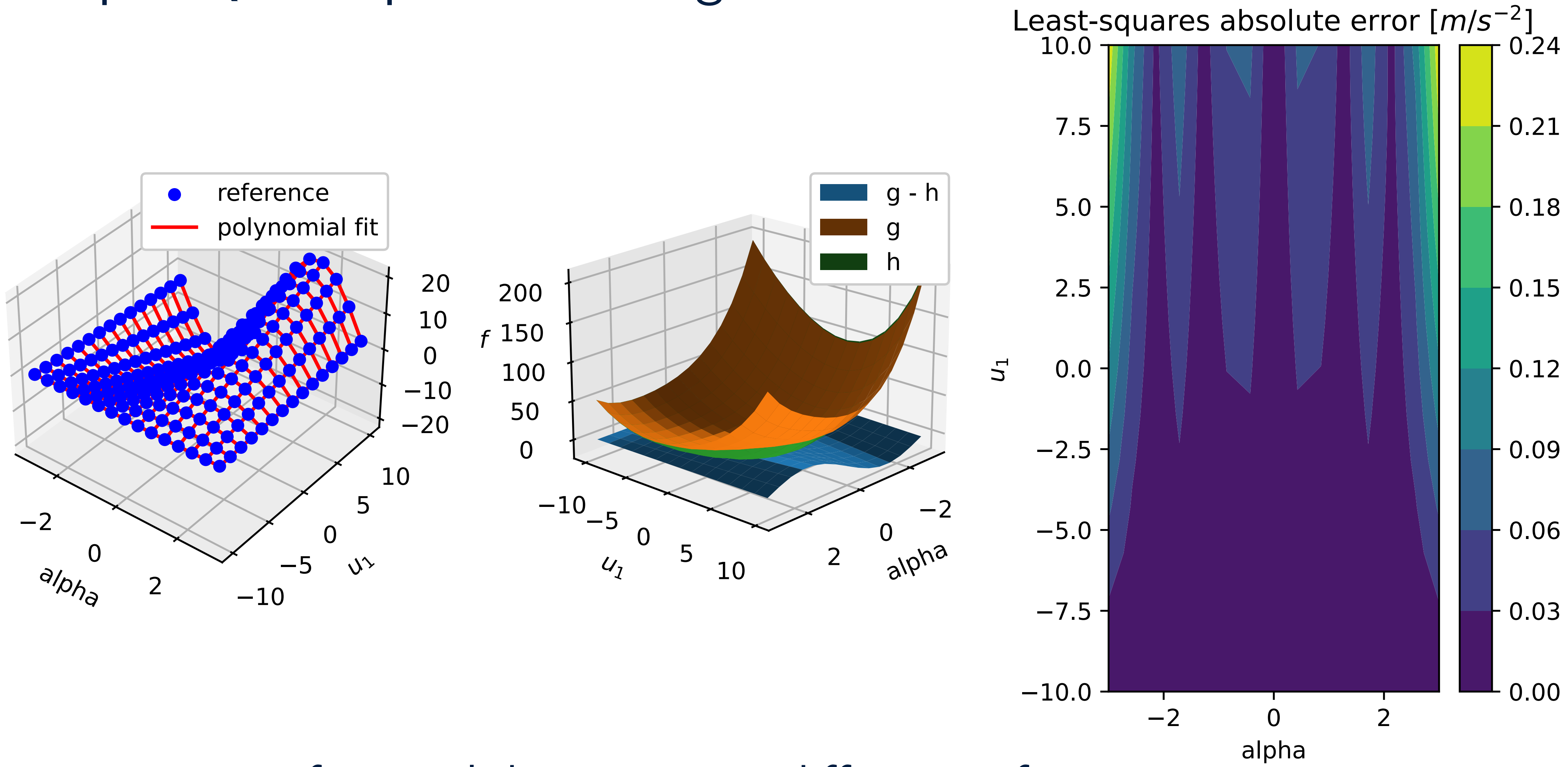

Approximation of vertical dynamics as a difference of convex polynomials

Example: Quadcopter modelling

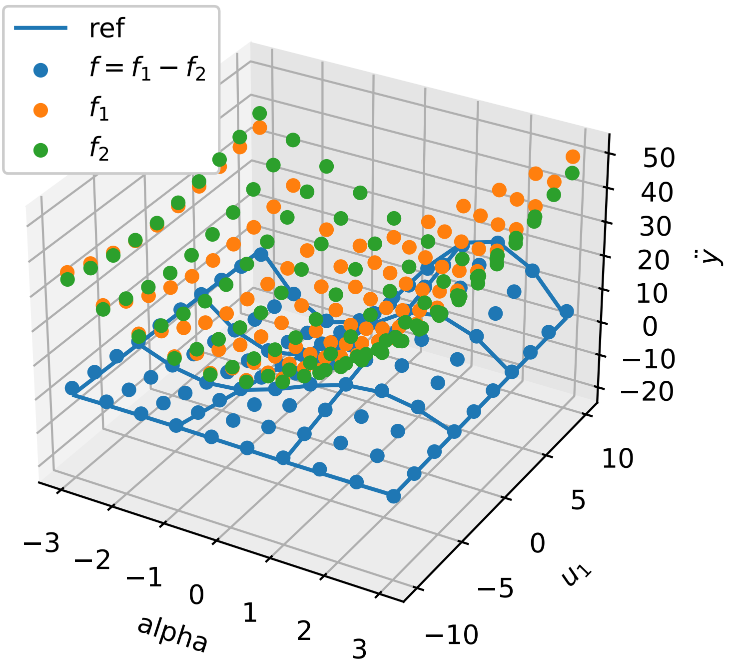

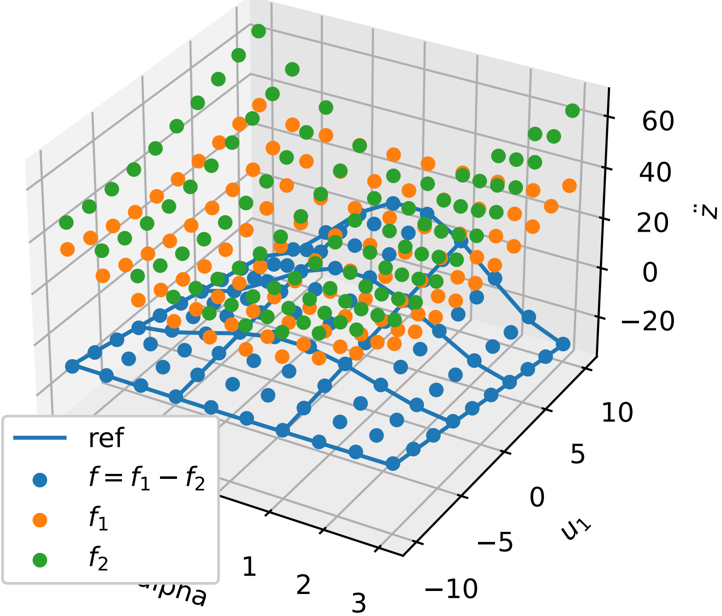

DCNN approximation of horizontal and vertical dynamics

Example: Quadcopter modelling

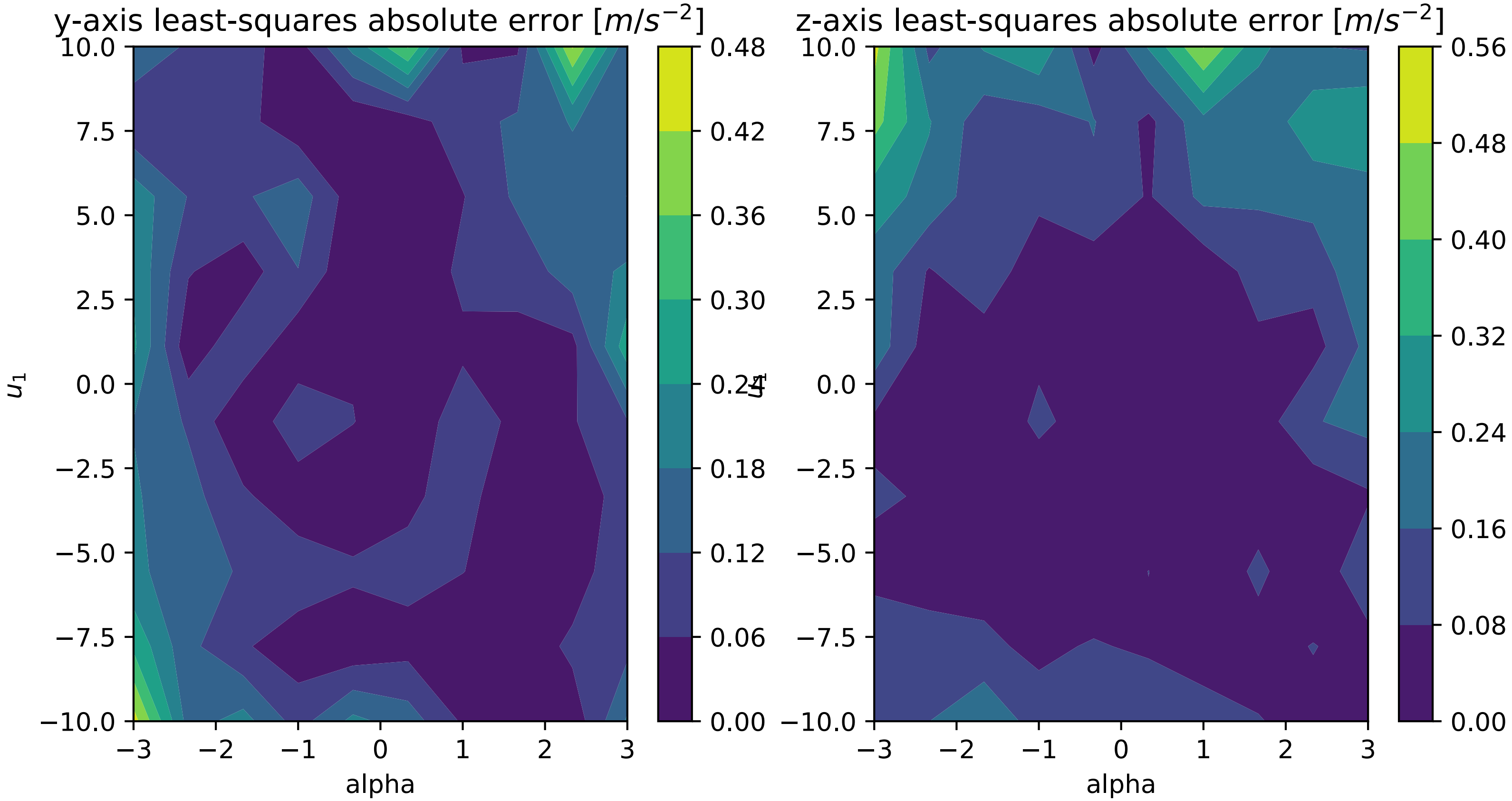

DCNN approximation of horizontal and vertical dynamics

Example: Quadcopter MPC

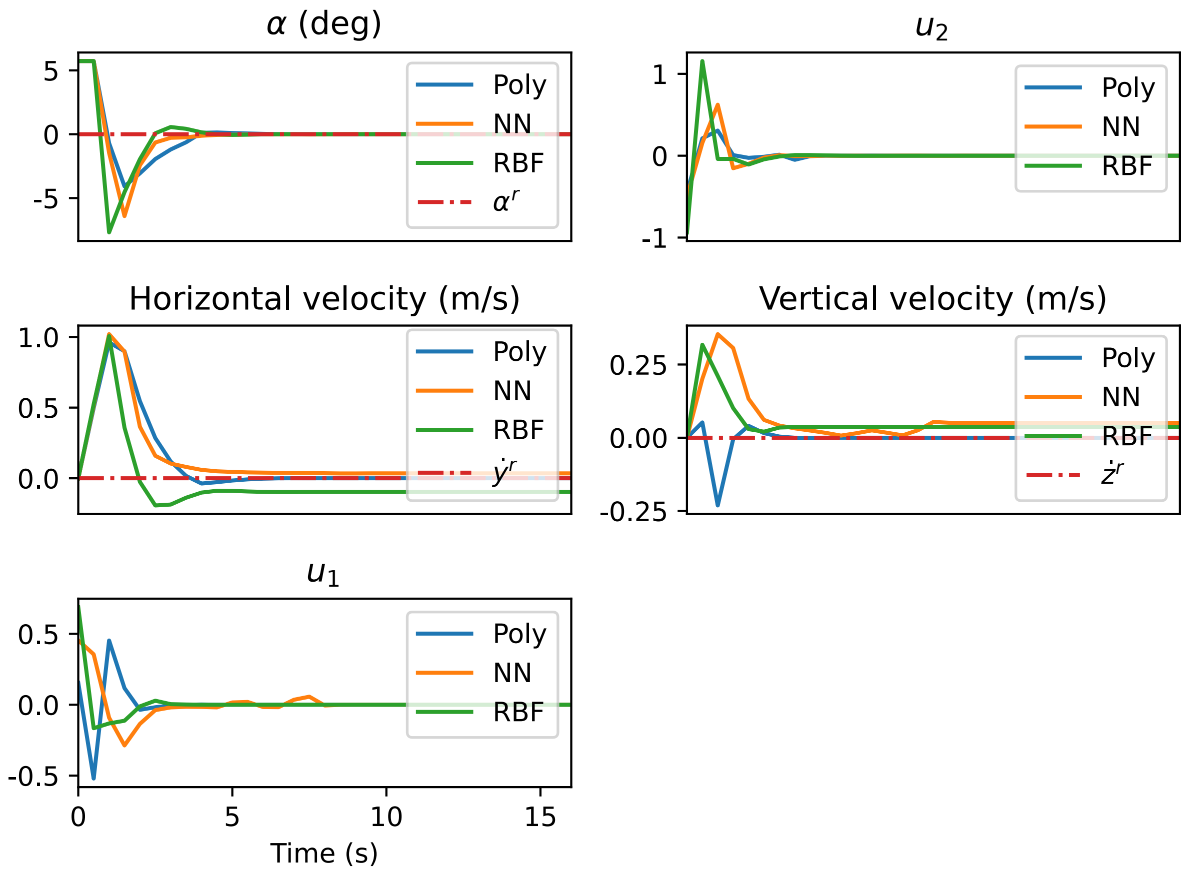

Control task is to regulate horizontal and vertical velocities, and pitch angle to zero

Comparison of closed loop responses for MPC with different DC model approximations

Polytopic, DCNN, and Radial Basis Functions

Outline

1. Recap: difference of convex (DC) tube (T)MPC via convex-concave procedure
2. Constructing DC models using polynomial approximations and ICNNs
3. Tube geometry is important!
4. Robustness to disturbances and recursive feasibility
5. Application examples:
   - tiltwing VTOL transition with wind-gust uncertainty
   - robust adaptive control of batch-fed bioreactor
   - data-driven control for closed loop deep brain stimulation

Tube geometry in MPC

Comparison of tube MPC strategies employing successive convexification

Ellipsoidal tube MPC

$\mathcal{X}_k = \{x : \|V(x - z_k)\|_2^2 \leq \beta_k^2\}$

Full model linearization;
robust constraint handling

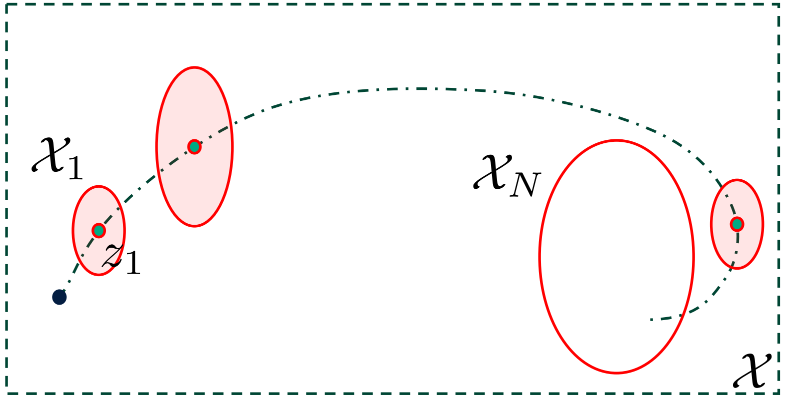

(e.g. Buerger, Cannon, ECC '25)

Tube geometry in MPC

Comparison of tube MPC strategies employing successive convexification

Ellipsoidal tube MPC

$\mathcal{X}_k = \{x : \|V(x - z_k)\|_2^2 \leq \beta_k^2\}$

Full model linearization;
robust constraint handling

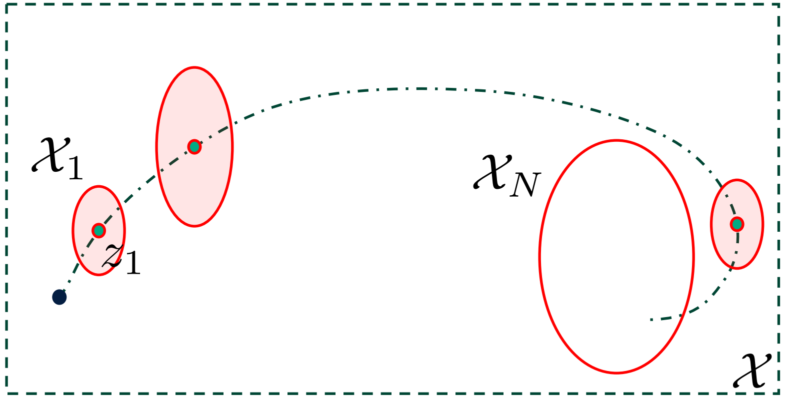

(e.g. Buerger, Cannon, ECC '25)

Hyperrectangular DC-TMPC

$\mathcal{X}_k = \{x : \underline{x}_k \leq x \leq \bar{x}_k\}$

Partial linearization of DC
model; robust constraints

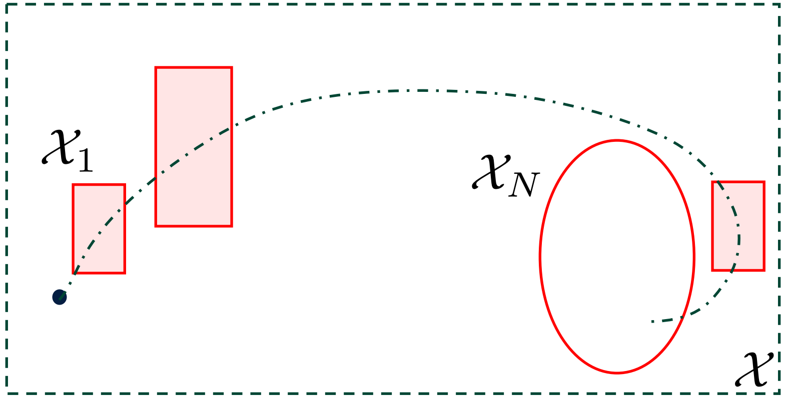

(e.g. Buerger, Cannon,
Doff-Sotta, L4DC '24)

Tube geometry in MPC

Comparison of tube MPC strategies employing successive convexification

Ellipsoidal tube MPC

$\mathcal{X}_k = \{x : \|V(x - z_k)\|_2^2 \le \beta_k^2\}$

Full model linearization; robust constraint handling

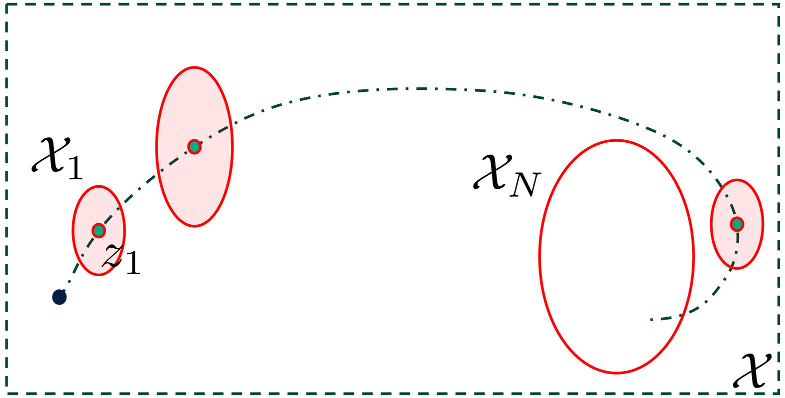

(e.g. Buerger, Cannon, ECC '25)

Hyperrectangular DC-TMPC

$\mathcal{X}_k = \{x : \underline{x}_k \le x \le \bar{x}_k\}$

Partial linearization of DC model; robust constraints

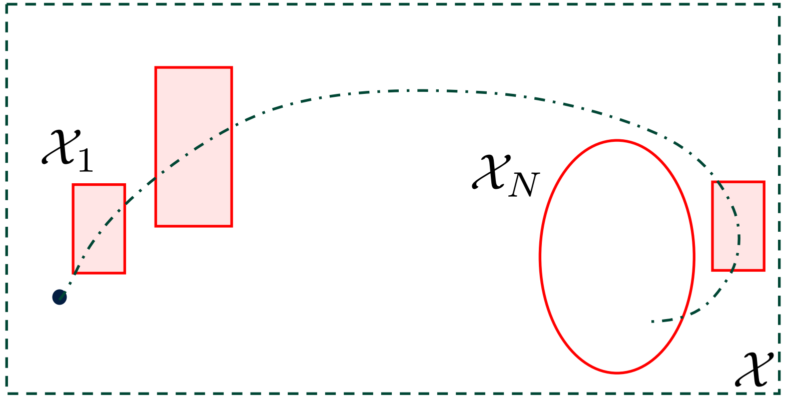

(e.g. Buerger, Cannon, Doff-Sotta, L4DC '24)

Simplex DC-TMPC

$\mathcal{X}_k = \{x : x \ge \underline{x}_k,\ \mathbf{1}^\top x \le \alpha_k\}$

Partial linearization of DC model; robust constraints

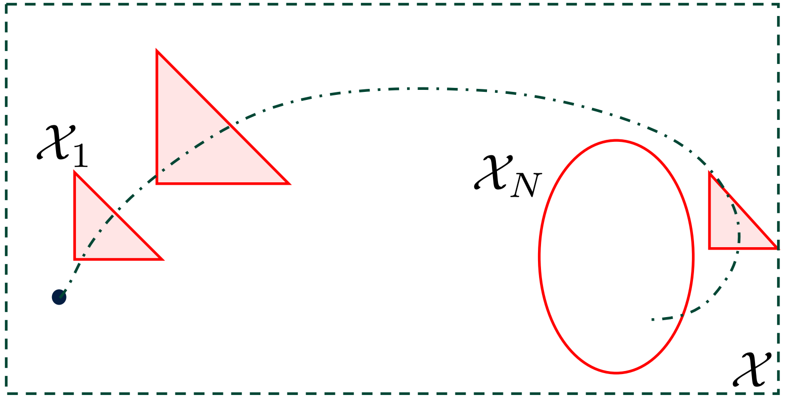

(e.g. Lishkova, Cannon, IEEE TAC '25)

Tube geometry in MPC

	Ellipsoid	Hyperrectangle	Simplex
Reachable set bounds	SOC constraints	Convex polynomial constraints	Convex polynomial constraints
Approximation error handling	Explicit bounds, e.g. local Lipchitz constants	Implicitly bounded	Implicitly bounded
#Extreme points of tube	$O(Nn_\theta)$	$O(2^{n_x} Nn_\theta)$	$O((n_x+1)Nn_\theta)$
Suboptimal with no additive disturbance?	Yes (depends on approx. error handling)	No (convergent to local optimum)	No (convergent to local optimum)
Convergence rate	Slow (depends on approx. error handling)	Fast	Slow if n_x is large
Potential for data-driven models	Low	High	High
Potential for online parameter adaptation	High	High	High

Effect of tube geometry on computation

- Monte Carlo simulations of systems with quadratic nonlinearities:

$$x_{k+1} = Ax_k + Bu_k + \sum_{i=1}^{n_\theta} \theta_i [x]_{j_i}^2 \hat{e}_i + w_k$$

$$w_k \in \mathcal{W} = \{B_w \hat{w} : \|\hat{w}\|_\infty \leq 0.01\}$$

  A, B, B_w, $j_i \in \{1, \dots, n_x\}$, Θ_0, and true parameter θ^* randomly generated

  Θ_t updated online using SME, $\theta_t^0 = \mathrm{centroid}(\Theta_t)$

- Compare:
  - Ellipsoidal tube MPC with full linearisation and explicit error bounding
  - DC-TMPC with hyperrectangle and simplex tube cross-sections

Effect of tube geometry on computation

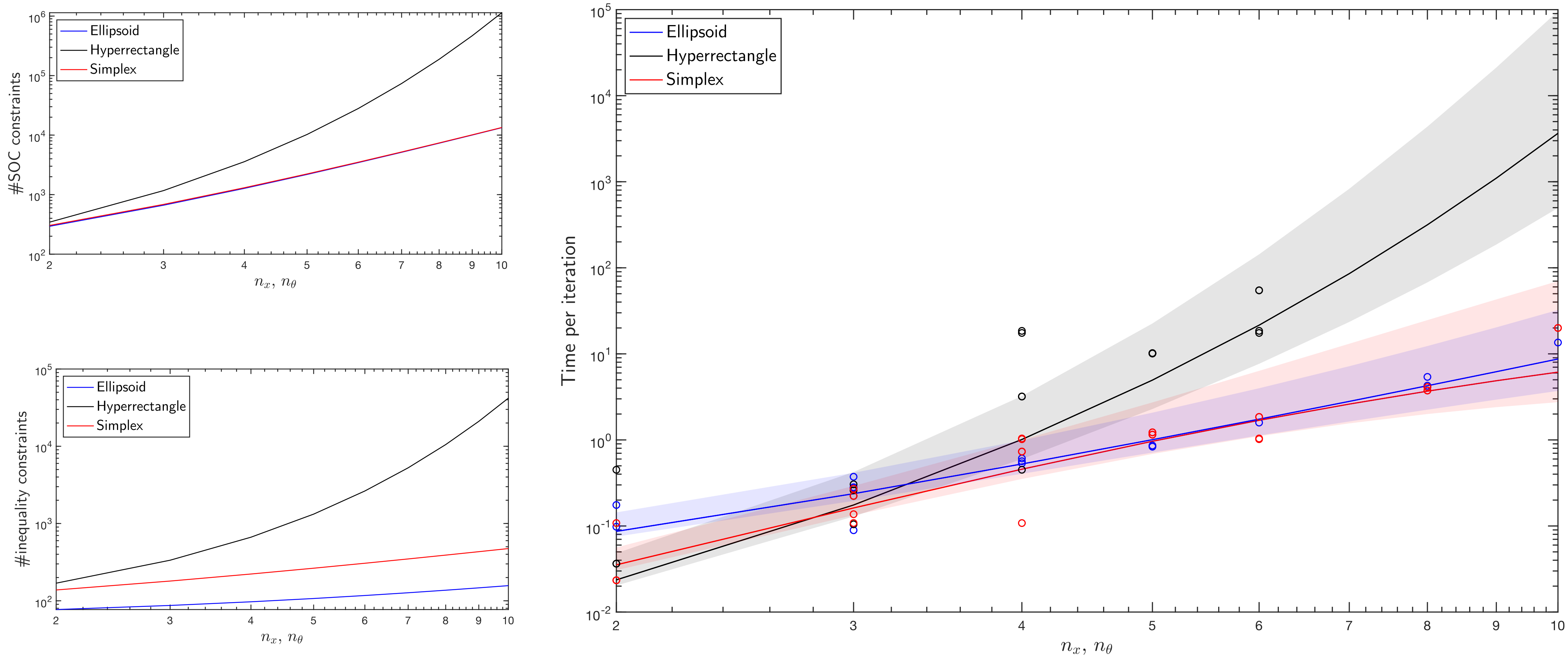

Time per iteration (mean and 90% confidence interval) determined using 10 random system models for each (n_x, n_θ) combination

Effect of tube geometry on computation

- Optimization solved using Gurobi (Apple M3 Pro, 36 GB memory)

  Dominant factor is #SOC constraints for all tube geometries

- #SOC constraints

Ellipsoidal tube:	$\sim n_x n_\theta^2 N$
Hyperrectangular tube:	$\sim 2^{n_x+1} n_\theta^2 N$
Simplex tube:	$\sim n_x n_\theta^2 N$

- Similar trends hold for higher order polynomial nonlinearities

Outline

1. Recap: difference of convex (DC) tube (T)MPC via convex-concave procedure
2. Constructing DC models using polynomial approximations and ICNNs
3. Tube geometry is important!
4. Robustness to disturbances and recursive feasibility
5. Application examples:
   - tiltwing VTOL transition with wind-gust uncertainty
   - robust adaptive control of batch-fed bioreactor
   - data-driven control for closed loop deep brain stimulation

Robust MPC nonlinear program

$$
\begin{aligned}
\mathcal{P}_t : \quad \underset{\mathbf{v},\mathbf{X}}{\text{minimize}} \quad & \max_{x \in \mathcal{X}_N} l_{\mathbb{T}}(x) + \sum_{k=0}^{N-1} \max_{x \in \mathcal{X}_k} l_k(x, Kx + v_k) \\
\text{s.t.} \quad & x_t^p \in \mathcal{X}_0 \\
& \mathcal{X}_N \subseteq \mathcal{X}_{\mathbb{T}} \\
& f(x, Kx + v_k) + w \in \mathcal{X}_{k+1}, \ \forall x \in \mathcal{X}_k, \ \forall w \in \mathcal{W} \\
& \mathcal{X}_k \subseteq \mathcal{X} \\
& K\mathcal{X}_k + v_k \subseteq \mathcal{U} \\
& \text{for } k = 0, \ldots, N-1
\end{aligned}
$$

- $\mathcal{W}$ assumed to be a bounded convex polytope, $\mathcal{W} = \text{co}\{w^{(1)}, \ldots, w^{(\nu)}\}$
- MPC law: $u_t^p = Kx_t + v_0^*$ at time t, where $(\mathbf{v}^*, \mathbf{X}^*)$ is a solution of $\mathcal{P}_t$

Robust DC-TMPC convex program

$$
\begin{aligned}
\hat{\mathcal{P}}_t : \quad \underset{\mathbf{v},\mathbf{X}}{\text{minimize}} \quad & \max_{x \in \mathcal{X}_N} l_{\mathbb{T}}(x) + \sum_{k=0}^{N-1} \max_{x \in \mathcal{X}_k} l_k(x, Kx + v_k) \\
\text{s.t.} \quad & x_t^p \in \mathcal{X}_0 \\
& \mathcal{X}_N \subseteq \mathcal{X}_{\mathbb{T}} \\
& \hat{f}_Q(x, Kx + v_k) + \bar{w} \leq q_{k+1} \; \forall x \in \mathcal{V}(\mathcal{X}_k) \\
& \mathcal{X}_k \subseteq \mathcal{X} \\
& K\mathcal{X}_k + v_k \subseteq \mathcal{U} \\
& \text{for } k = 0, \ldots, N-1
\end{aligned}
$$

- Convex approximation $\hat{f}_Q$
- Robust terminal set $\mathcal{X}_{\mathbb{T}}$ and terminal cost $l_{\mathbb{T}}$

Robust DC-TMPC sequential convex program

Input: $(\mathbf{x}^\circ, \mathbf{v}^\circ)$ satisfying: $x_0^\circ = x_t^p$, $\mathcal{X}_N^\circ \subseteq \mathcal{X}_\mathbb{T}$, $K\mathcal{X}_k^\circ + v_k^\circ \subseteq \mathcal{U}$, $\mathcal{X}_k^\circ \subseteq \mathcal{X}$,
$x_{k+1}^\circ = f(x_k^\circ, Kx_k^\circ + v^\circ)$, $\mathcal{X}_{k+1}^\circ \supseteq f(\mathcal{X}_k^\circ, K\mathcal{X}_k^\circ + v_k^\circ) + \mathcal{W}$, $\forall k$

Iteration: set $i \leftarrow 0$ $J_t^{(-1)} \leftarrow \infty$, $\mathit{flag} \leftarrow 1$

while flag

solve $\hat{\mathcal{P}}_t$ and set $J_t^{(i)} \leftarrow \mathrm{value}(\hat{\mathcal{P}}_t)$
$(\mathbf{v}^{(i)}, \mathbf{X}^{(i)}) \leftarrow (\mathbf{v}^*, \mathbf{X}^*)$
$i \leftarrow i + 1$

update $(\mathbf{x}^\circ, \mathbf{u}^\circ)$: $u_k^\circ \leftarrow Kx_k^\circ + v_k^*$
$x_{k+1}^\circ \leftarrow f(x_k^\circ, u_k^\circ)$, $k = 0, \dots N-1$

if $i \geq \mathit{maxiters}$ or $J_t^{(i-2)} - J_t^{(i-1)} < \mathit{tolerance}$
set $\mathit{flag} \leftarrow 0$

Output: $\{u_0^*, \dots, u_{N-1}^*\}$, $\{x_0^*, \dots, x_N^*\}$, $\mathrm{value}(\hat{P}_t)$

MPC algorithm at time t

$i \leftarrow 0$, $x_t^p \leftarrow$ plant state at time t

↓

Compute $\mathbf{x}^\circ, \mathbf{u}^\circ$ given $\mathbf{v}^\circ$
$\hat{f}_Q \leftarrow$ linearize concave component at $\mathbf{x}^\circ, \mathbf{u}^\circ$
Solve $\hat{\mathcal{P}}_t$ for $\mathbf{v}^*, \mathbf{X}^*$

MPC algorithm at time t

$i \leftarrow 0$, $x_t^p \leftarrow$ plant state at time t

↓

Compute $\mathbf{x}^\circ, \mathbf{u}^\circ$ given $\mathbf{v}^\circ$
$\hat{f}_Q \leftarrow$ linearize concave component at $\mathbf{x}^\circ, \mathbf{u}^\circ$
Solve $\hat{\mathcal{P}}_t$ for $\mathbf{v}^*, \mathbf{X}^*$

↓

If $\|\mathbf{v}^*\| < \mathrm{tol}$ or $i \geq \mathrm{maxIter}$:

$\mathbf{v}^\circ_{\mathrm{old}} \leftarrow \mathit{shift}_u(\mathbf{v}^\circ)$
$\mathbf{x}^\circ_{\mathrm{old}} \leftarrow \mathit{shift}_x(\mathbf{x}^\circ)$
$\mathbf{v}^\circ \leftarrow \mathit{shift}_u(\mathbf{v}^*)$
apply control $u_t = K x_t^p + v_0^*$

$$\mathit{shift}_u(\mathbf{v}) \triangleq \{v_1, \ldots, v_{N-1}, 0\}$$
$$\mathit{shift}_x(\mathbf{x}) \triangleq \{x_1, \ldots, x_N, f_K(x_N, 0; \theta^0)\}$$

MPC algorithm at time t

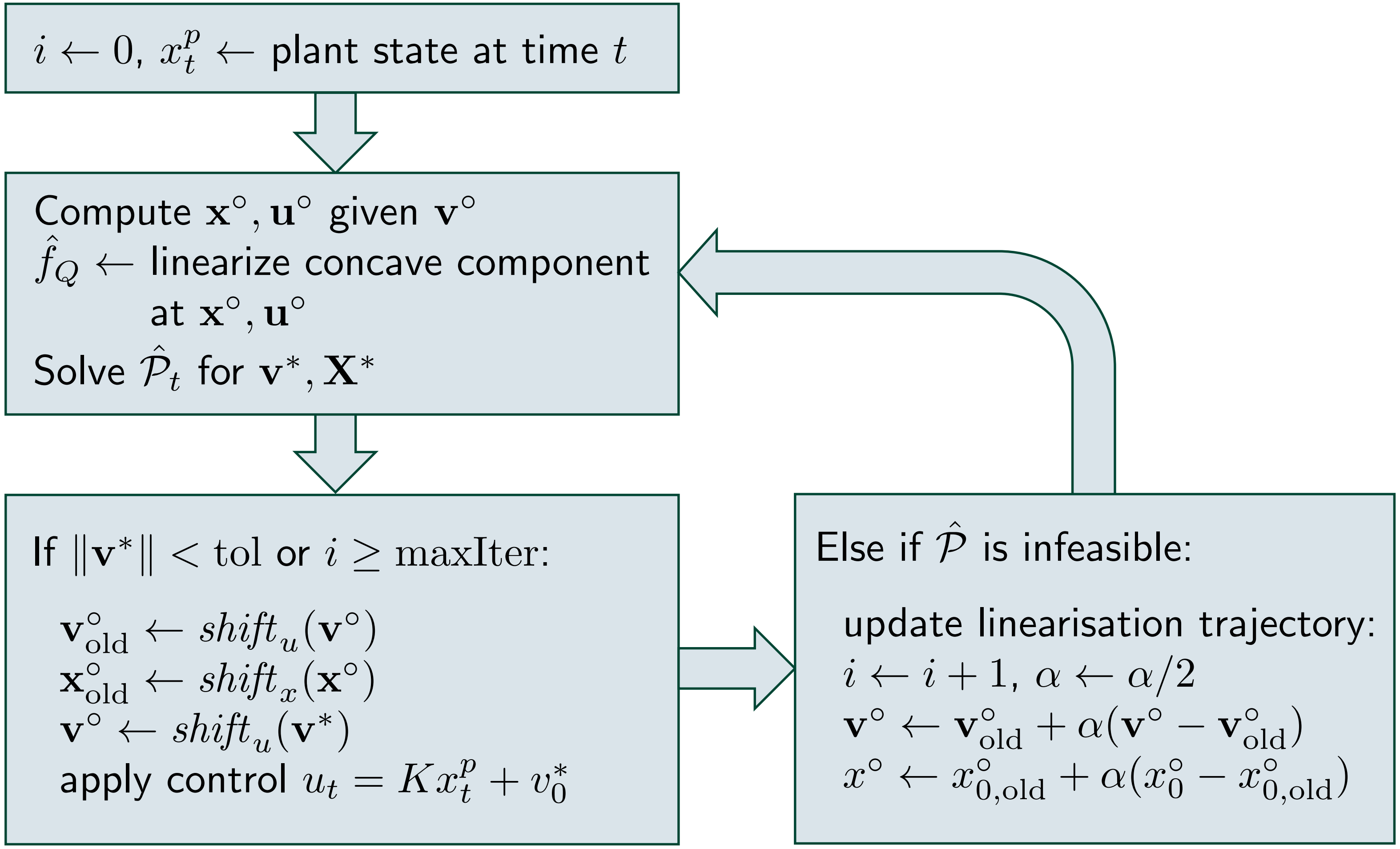

$$\mathit{shift}_u(\mathbf{v}) \triangleq \{v_1, \ldots, v_{N-1}, 0\}$$
$$\mathit{shift}_x(\mathbf{x}) \triangleq \{x_1, \ldots, x_N, f_K(x_N, 0; \theta^0)\}$$

MPC algorithm at time t

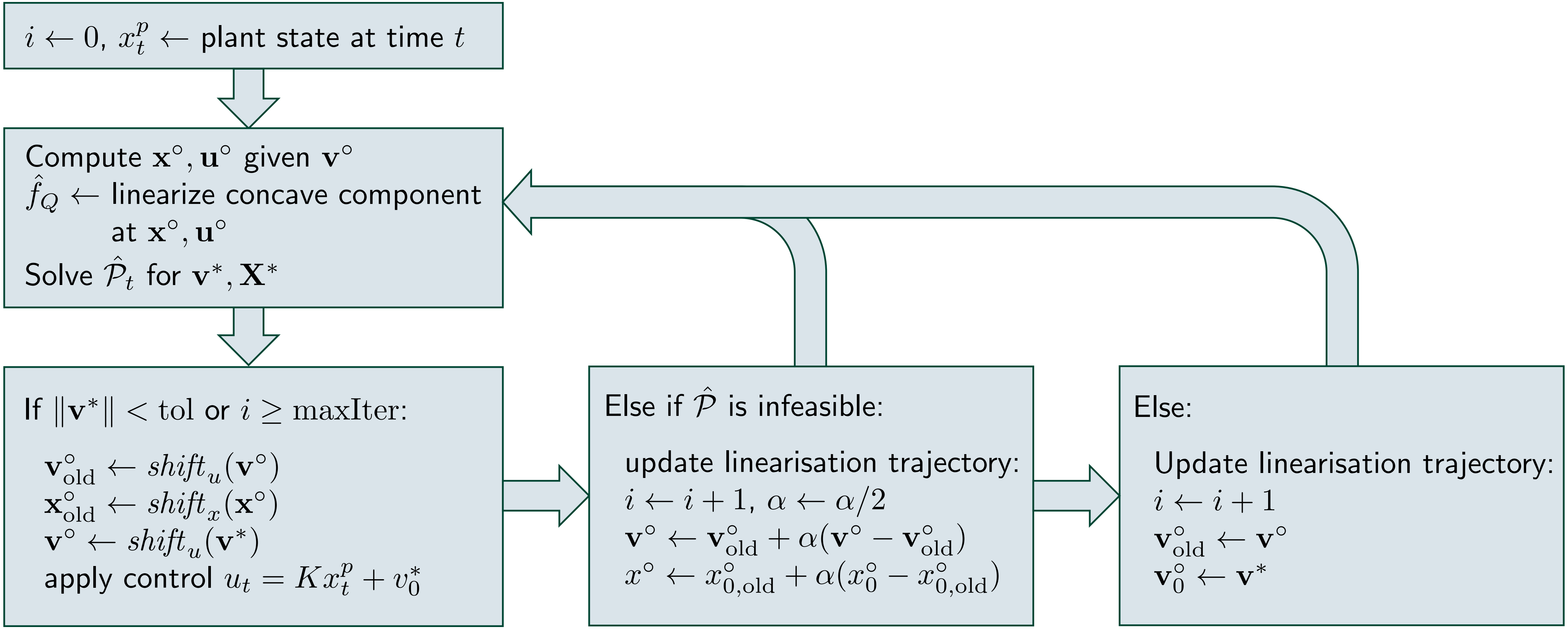

$$\mathit{shift}_u(\mathbf{v}) \triangleq \{v_1, \ldots, v_{N-1}, 0\}$$
$$\mathit{shift}_x(\mathbf{x}) \triangleq \{x_1, \ldots, x_N, f_K(x_N, 0; \theta^0)\}$$

Outline

1. Recap: difference of convex (DC) tube (T)MPC via convex-concave procedure
2. Constructing DC models using polynomial approximations and ICNNs
3. Tube geometry is important!
4. Robustness to disturbances and recursive feasibility
5. Application examples:
   - tiltwing VTOL transition with wind-gust uncertainty
   - robust adaptive control of batch-fed bioreactor
   - data-driven control for closed loop deep brain stimulation

Robust MPC: eVTOL aircraft

- Light electric aircraft for short flights

  Aim to reduce congestion and air pollution in cities

- Control challenges: robust trajectory optimization & control during transitions

Rolls-Royce eVTOL prototype

Transition between vertical and horizontal flight

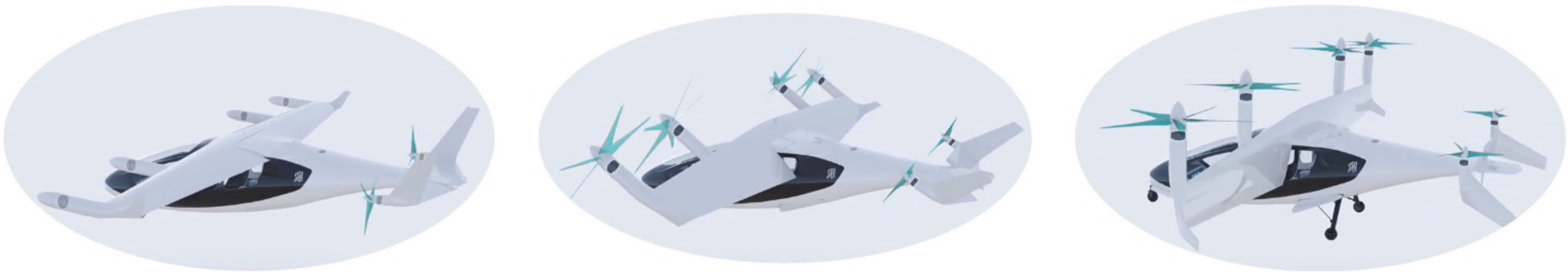

Forward/backward transition manoeuvre for tiltwing VTOL aircraft

Control Problem:

Track a reference trajectory for a tiltwing VTOL aircraft transition between wing-borne and thrust-borne flight subject to state and control constraints, model uncertainty and unknown wind gusts

Tiltwing VTOL aircraft model

Model of (x, z)-plane motion

$$m\dot{v}_x = T\cos(\alpha+\gamma) - D\cos\gamma - L\sin\gamma + w_x,$$
$$m\dot{v}_z = -T\sin(\alpha+\gamma) + D\sin\gamma - L\cos\gamma + mg + w_z,$$
$$J\ddot{i}_w = M$$
$$i_w + \theta = \gamma + \alpha$$

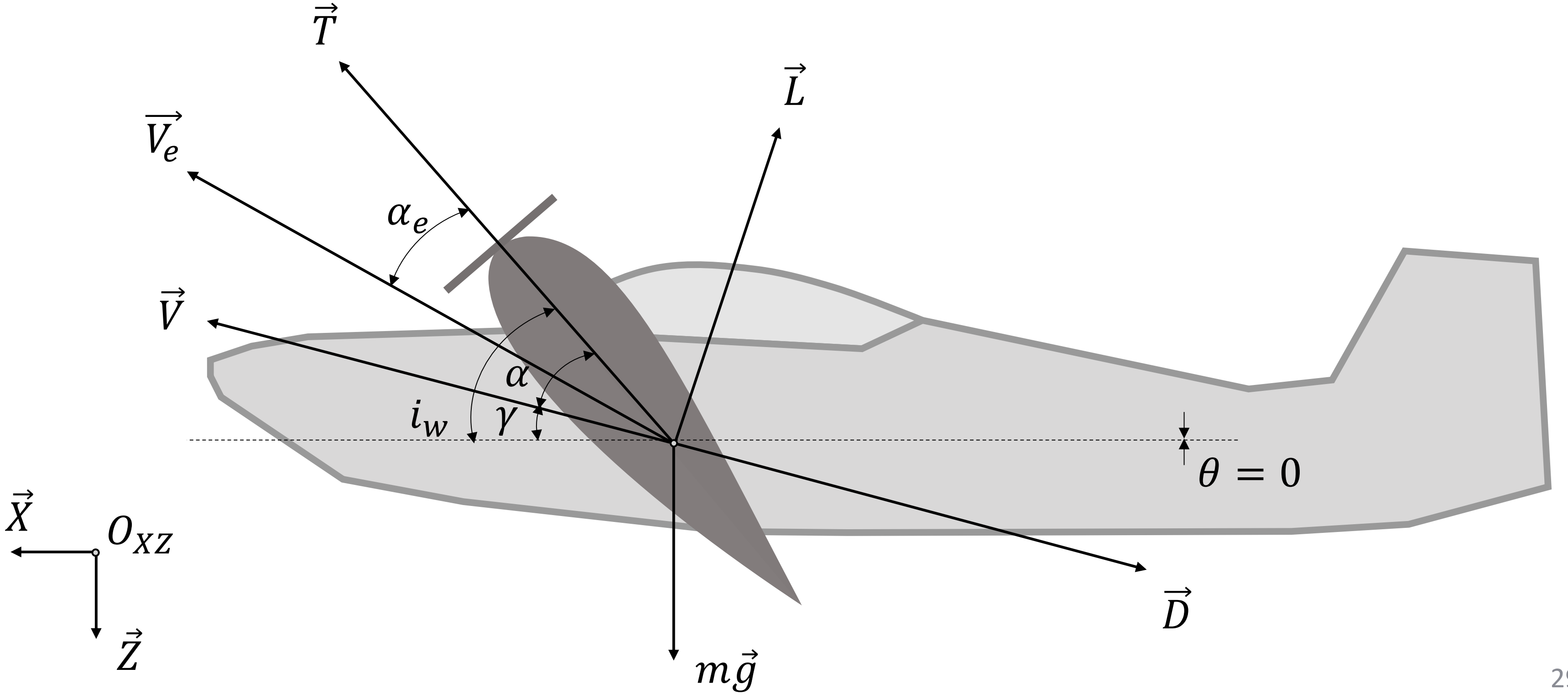

Tiltwing VTOL aircraft model

- Effective (blown) velocity V_e and effective (blown) angle of attack α_e seen by the wing due to the effect of the propeller wake on the wing:

$$\alpha_e = \arcsin\left(\frac{V}{V_e}\sin\alpha\right)$$

$$V_e = \sqrt{V^2 + \frac{2T}{\rho A n}}$$

- Total lift and drag are weighted sums of blown and unblown components:

$$L = \tfrac{1}{2}\lambda\rho S C_L(\alpha_e)V_e^2 + \tfrac{1}{2}(1-\lambda)\rho S C_L(\alpha)V^2,$$
$$D = \tfrac{1}{2}\lambda\rho S C_D(\alpha_e)V_e^2 + \tfrac{1}{2}(1-\lambda)\rho S C_D(\alpha)V^2,$$

Tiltwing VTOL aircraft model

To allow a wide range of angles of attack α, α_e, the lift and drag coefficients $C_L(\cdot), C_D(\cdot)$ are obtained using the Tangler-Ostowari post-stall model

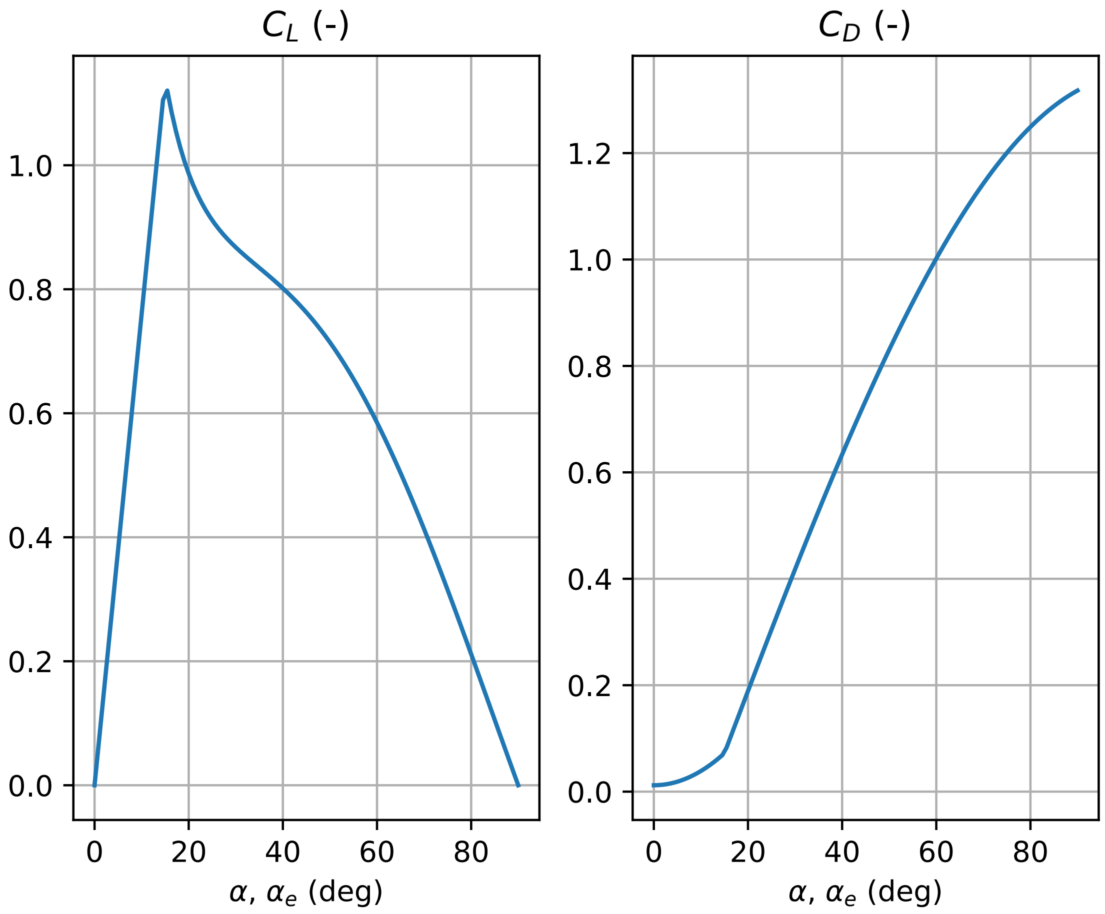

Disturbances and constraints

- Bounds on wind gust disturbances

$$\underline{w}_x \leq w_x \leq \bar{w}_x, \quad \underline{w}_z \leq w_z \leq \bar{w}_z$$

- Constraints on states v_x, v_z and control inputs T, M:

$$\begin{bmatrix} \underline{v}_x \\ \underline{v}_z \end{bmatrix} \leq \begin{bmatrix} v_x \\ v_z \end{bmatrix} \leq \begin{bmatrix} \bar{v}_x \\ \bar{v}_z \end{bmatrix}$$

$$\begin{matrix} 0 \leq T \leq \bar{T} \\ \underline{i}_w \leq i_w \leq \bar{i}_w \end{matrix} \qquad \begin{bmatrix} \underline{a}_x \\ \underline{a}_z \end{bmatrix} \leq \begin{bmatrix} \dot{v}_x \\ \dot{v}_z \end{bmatrix} \leq \begin{bmatrix} \bar{a}_x \\ \bar{a}_z \end{bmatrix} \qquad \underline{M}/J_w \leq \ddot{i}_w \leq \overline{M}/J_w$$

DC model approximation

- DC decomposition: $f_1 = g_1 - h_1$, $f_2 = g_2 - h_2$:

$$m\dot{v_x} = g_1(v_x, v_z, i_w, T) - h_1(v_x, v_z, i_w, T) + w_x,$$
$$m\dot{v_z} = g_2(v_x, v_z, i_w, T) - h_2(v_x, v_z, i_w, T) + w_z,$$

- Controller parameterisation with: optimization variables μ, τ
  feedback gains $K_{i_w}, K'_{i_w}, K_T, K'_T$

$$i_w = \mu + K_{i_w}(v_x - v_x^\circ) + K'_{i_w}(v_z - v_z^\circ),$$
$$T = \tau + K_T(v_x - v_x^\circ) + K'_T(v_z - v_z^\circ),$$

- Feasible initial guess trajectories $v_x^\circ, v_z^\circ, \mu^\circ, \tau^\circ$ obtained using DC-TMPC

DC model approximation

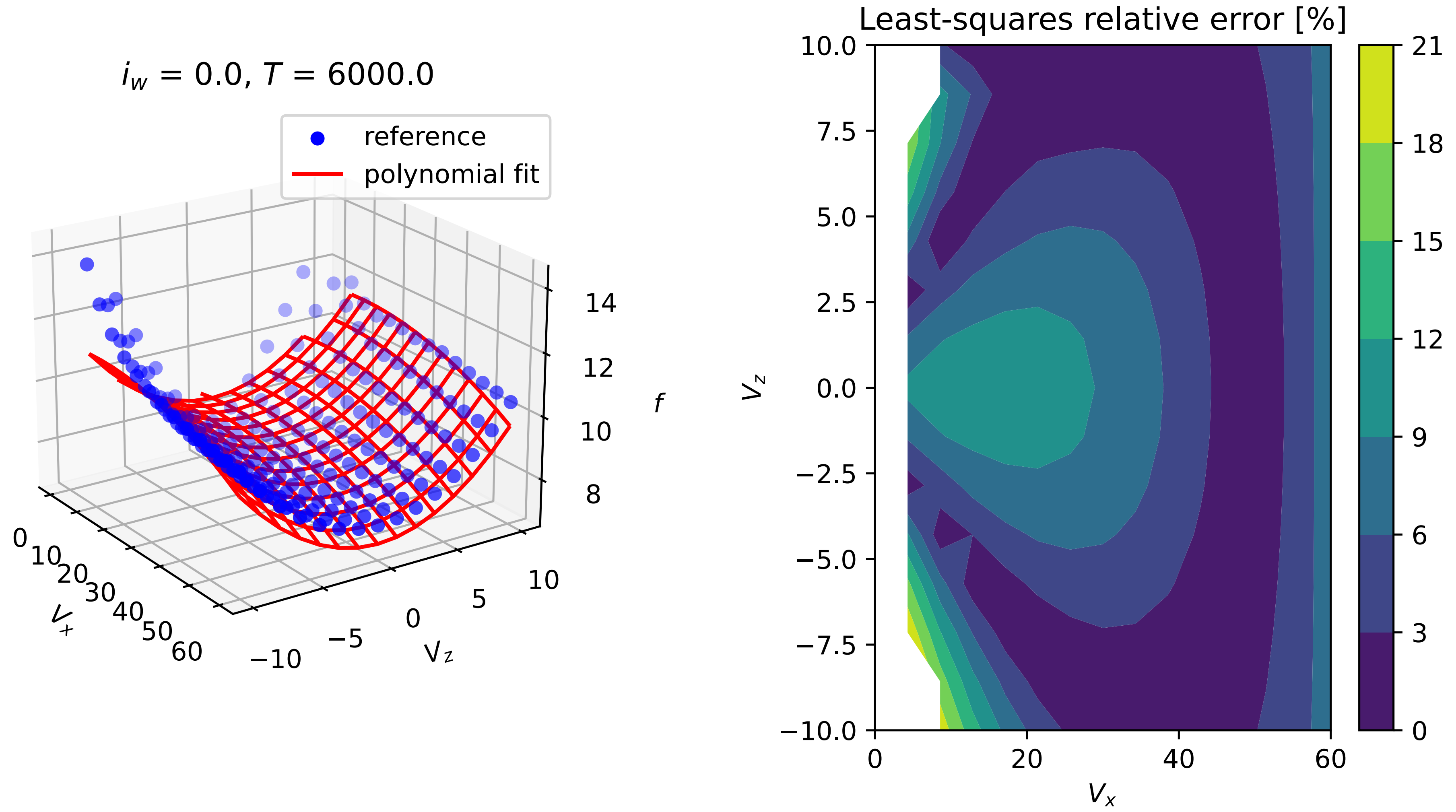

Least-squares fit of f_1 as a function of (V_x, V_z) for given i_w, T

Forward transition with no wind gusts

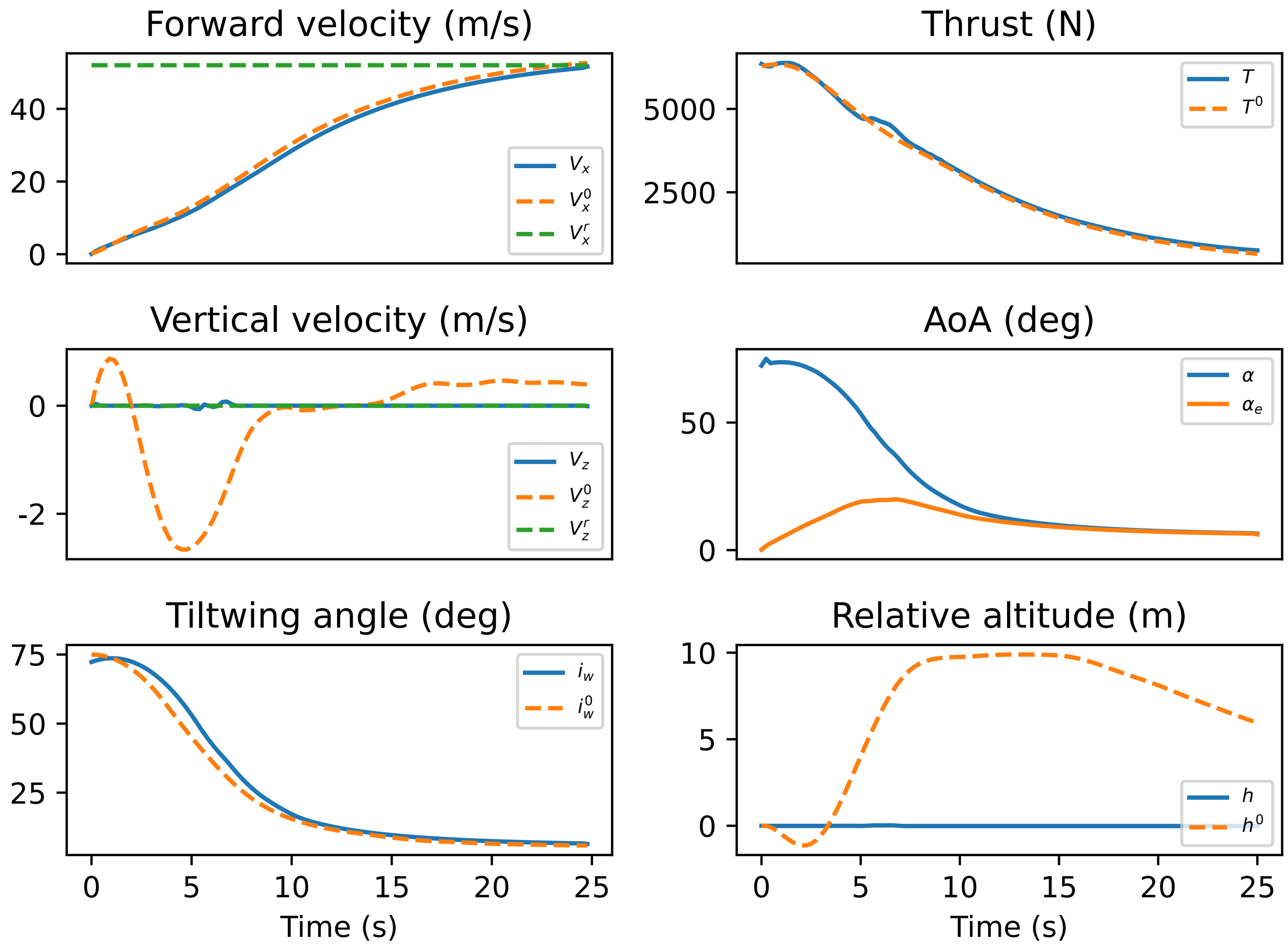

Constant altitude forward transition

Robustness to wind gust uncertainty

Gust perpendicular to direction of path affects L, D, α, α_e
EASA VTOL safety guidelines discrete wind gust velocity profile:

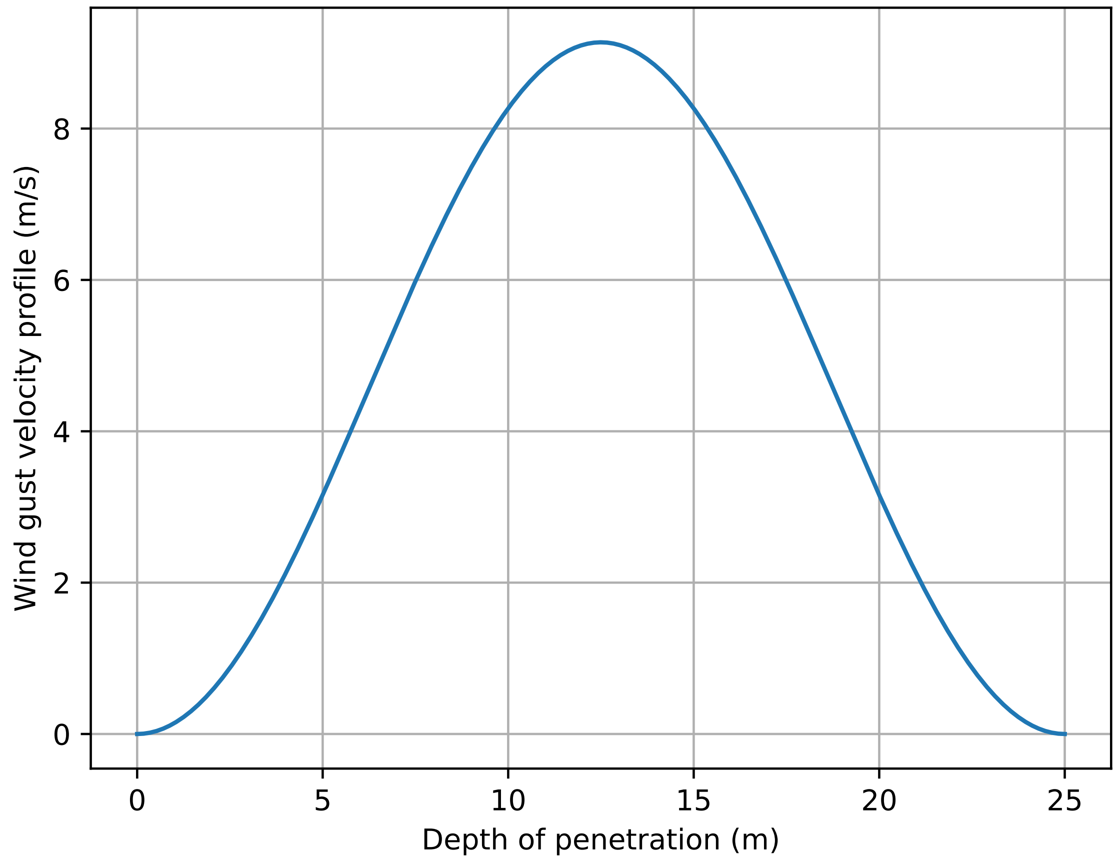

Design gust velocity $9.1\,\mathrm{m\,s^{-1}}$

Wind gust during forward transition

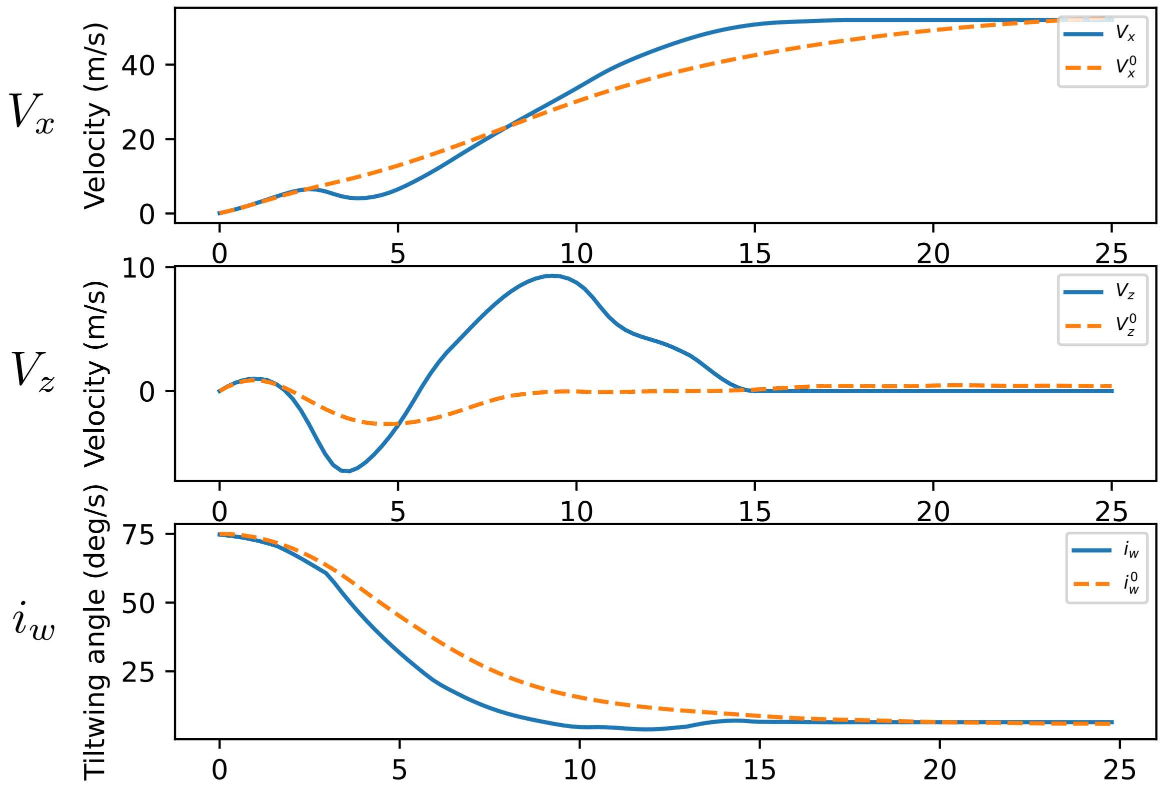

Gust at $0\,$s

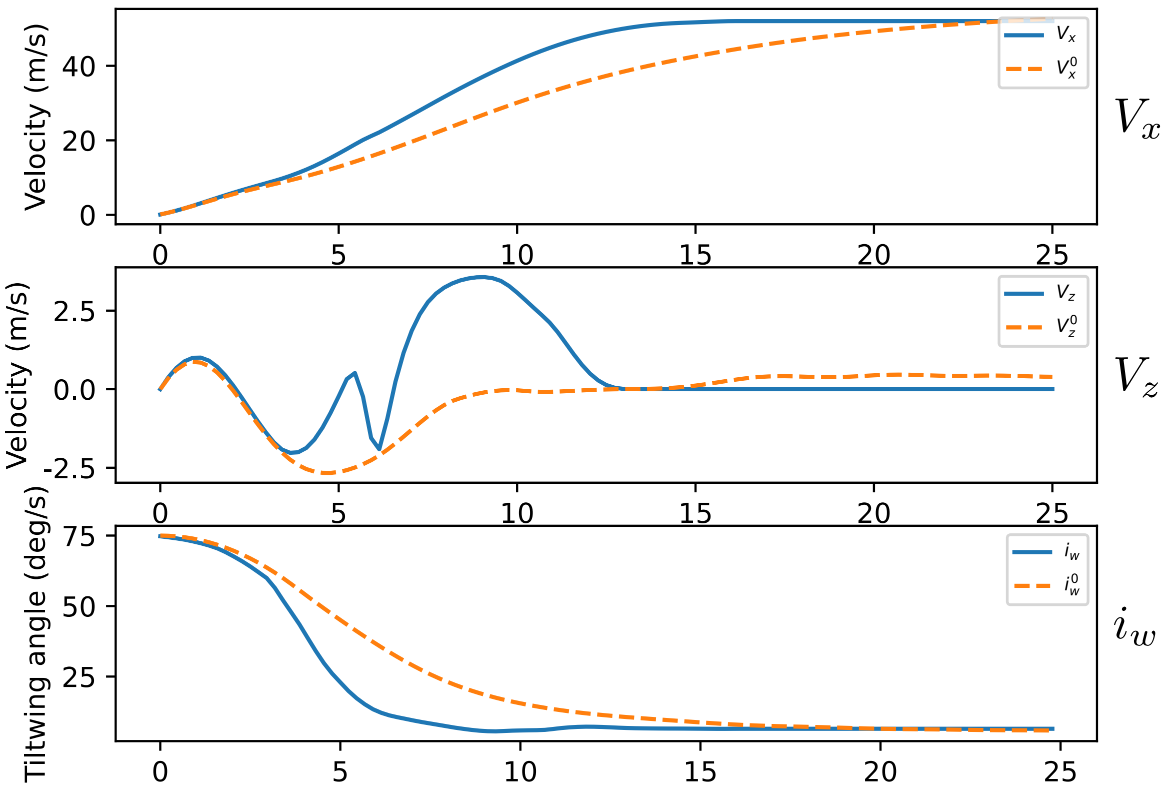

Gust at $5\,$s

Robustness to wind uncertainty demonstrated in forward and backward transitions

Outline

1. Recap: difference of convex (DC) tube (T)MPC via convex-concave procedure
2. Constructing DC models using polynomial approximations and ICNNs
3. Tube geometry is important!
4. Robustness to disturbances and recursive feasibility
5. Application examples:
   - tiltwing VTOL transition with wind-gust uncertainty
   - robust adaptive control of batch-fed bioreactor
   - data-driven control for closed loop deep brain stimulation

Adaptive MPC: Batch-fed Bioreactor

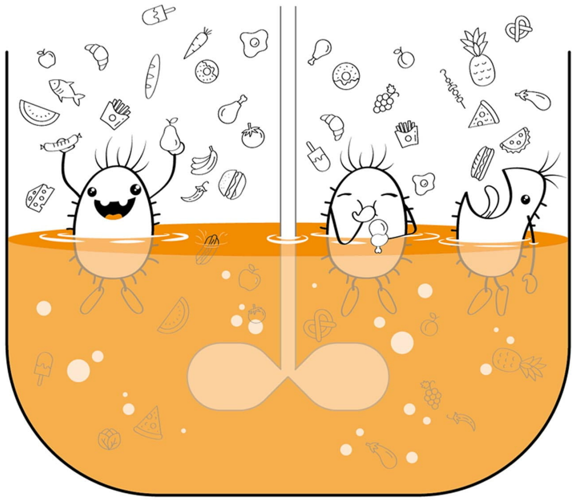

- Bioprocesses have nonlinear and uncertain dynamics

  MPC computational demand reduced via:
  - differences of convex function dynamic models
  - robust constrained tube MPC
  - convex optimization
- Models are nonlinear with uncertain parameters due to phenotypic variation
- Aim is to maximize product formation and learn model parameters online

Batch-fed Bioreactor

Model state: $x = (X, S, P, V)$, cell, product, substrate concentrations, volume

Control input: u, feed flow rate of substrate at concentration S_i

Objective: maximize $P(T)$

Dynamics:

$$\dot{X} = \mu(S)X - \frac{u}{V_0 + V}X$$

$$\dot{S} = -\mu(S)\frac{X}{Y_{X/S}} - v\frac{X}{Y_{P/S}} + \frac{u}{V_0 + V}(S_i - S)$$

$$\dot{P} = vX - \frac{u}{V_0 + V}P$$

$$\dot{V} = u$$

$$\mu(S) = \mu_{\max}\frac{S}{S + K_S + S^2/K_i}$$

unknown parameters $Y_{X/S}, S_i$

Batch-fed Bioreactor

- Model structure:

$$x_{t+1} = f(x_t, u_t) + F(x_t, u_t)\theta + w_t, \quad w_t \in \mathcal{W}, \quad \theta \in \Theta_t$$

- DC decomposition, g, h, G, H elementwise convex

$$f = g - h, \quad F = G - H,$$

- Set membership estimation (SME) parameter set update:

$$\Theta_{t+1} = \arg\min\ |\Theta| \ \text{ subject to } \ \Theta \supseteq \Theta_t \cap \Delta_{t+1}$$
$$\Delta_{t+1} = \{\theta : x_{t+1} - f(x_t, u_t) - F(x_t, u_t)\theta \in \mathcal{W}\}$$

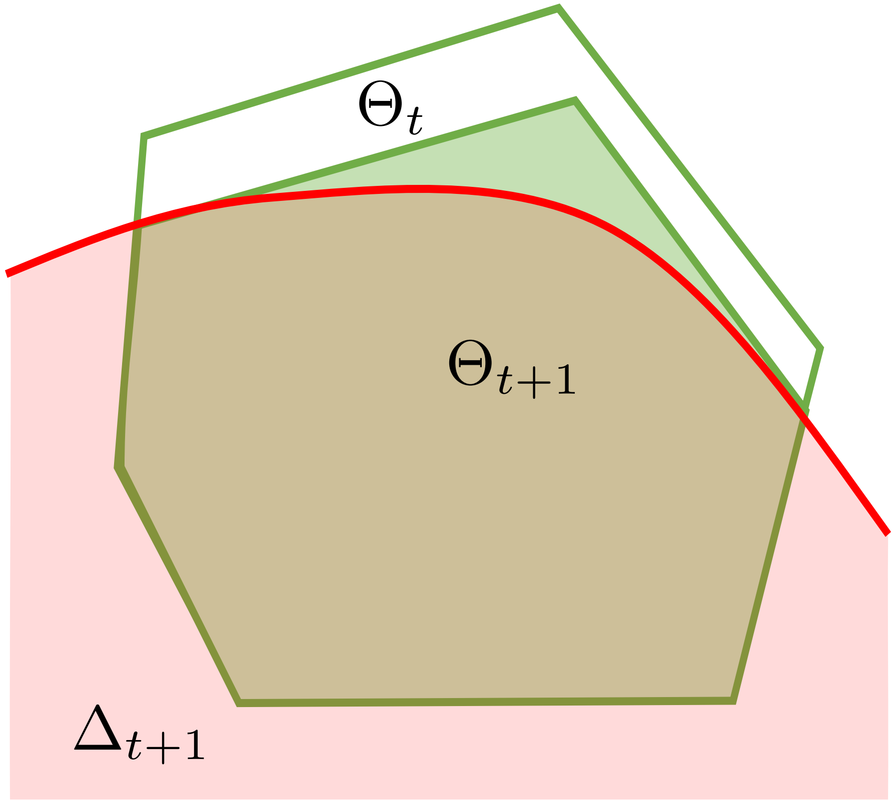

Batch-fed Bioreactor

- 2 DC NNs with ReLU activation functions modelling:
  - nominal dynamics
  - dependence on unknown parameters
- Trained using experimental data and phenomenological models

DC decomposition, $P =$ 0.4 g L^{-1}, $V =$ 122.0 L, $u =$ 0.07 L h^{-1}

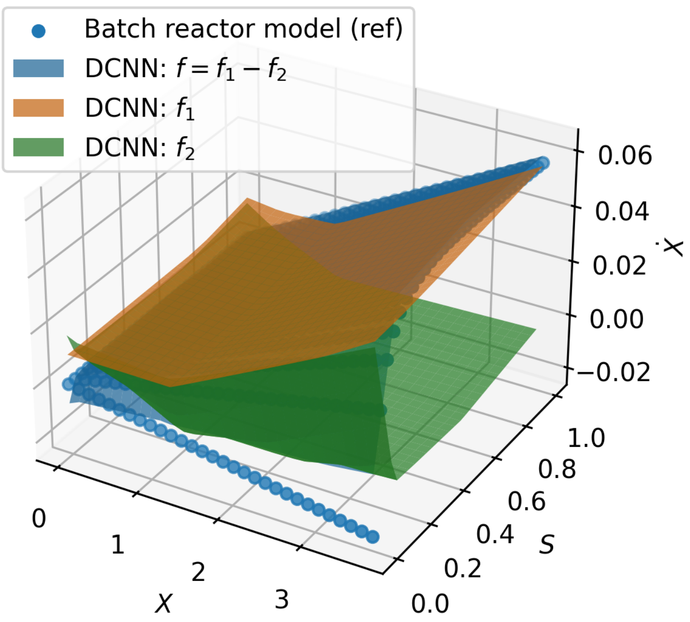

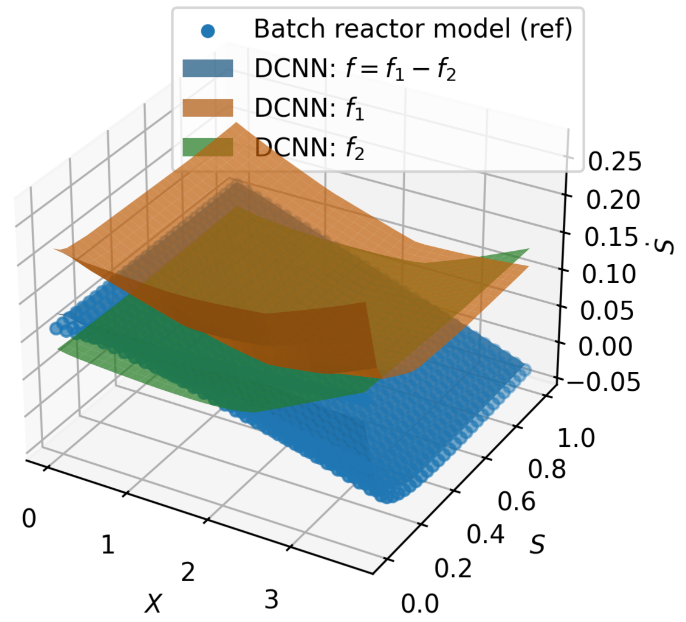

Batch-fed Bioreactor

- Predicted trajectories at initial time
- Successive convexification iteration
- Robust state tubes
- State and control constraints

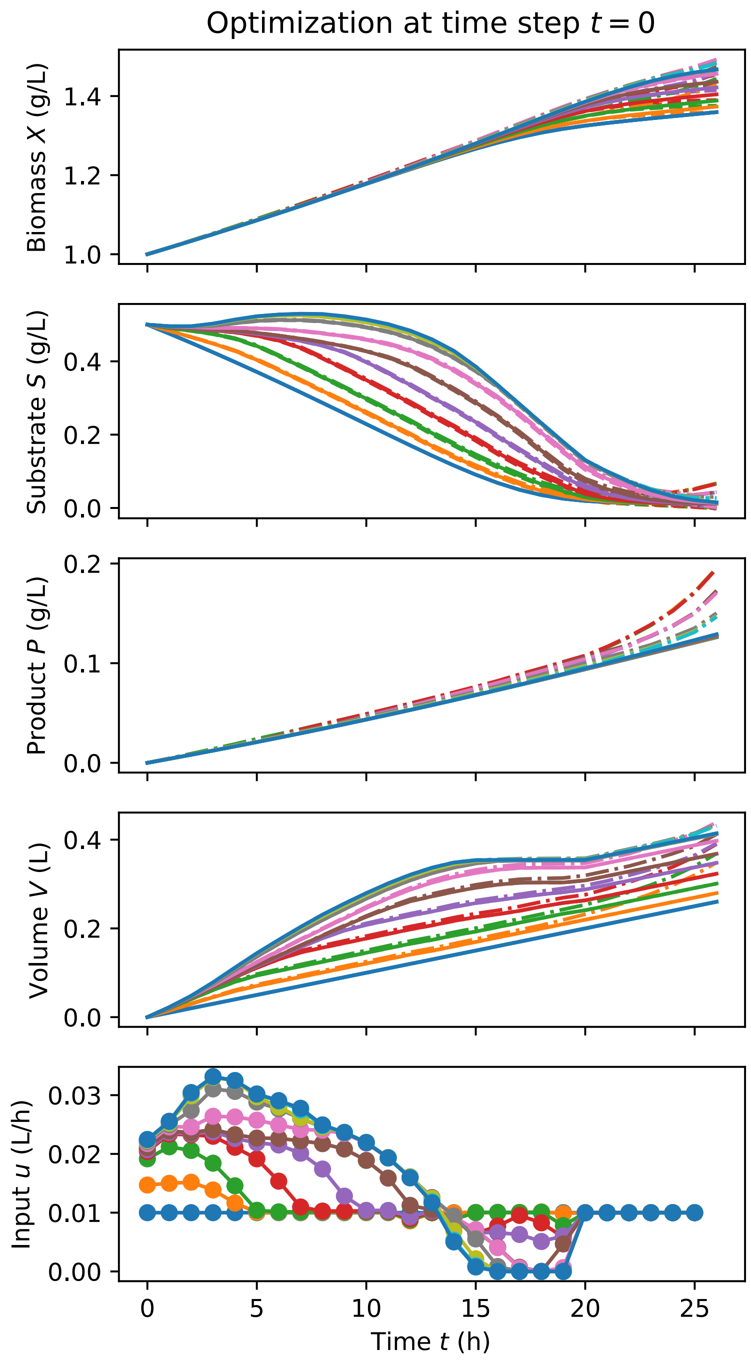

Batch-fed Bioreactor

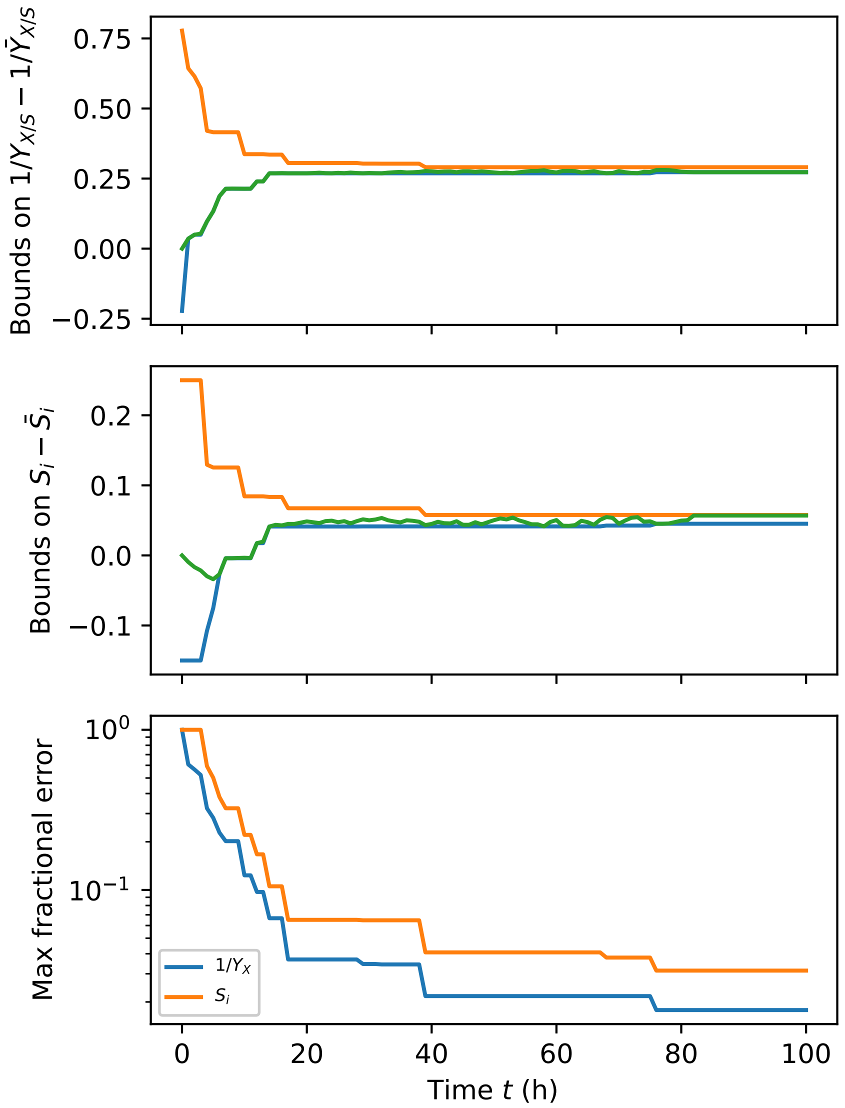

- Parameter estimates:
  - SME bounds
  - LS point estimates

- Closed loop responses

- 33% yield improvement due to parameter estimation

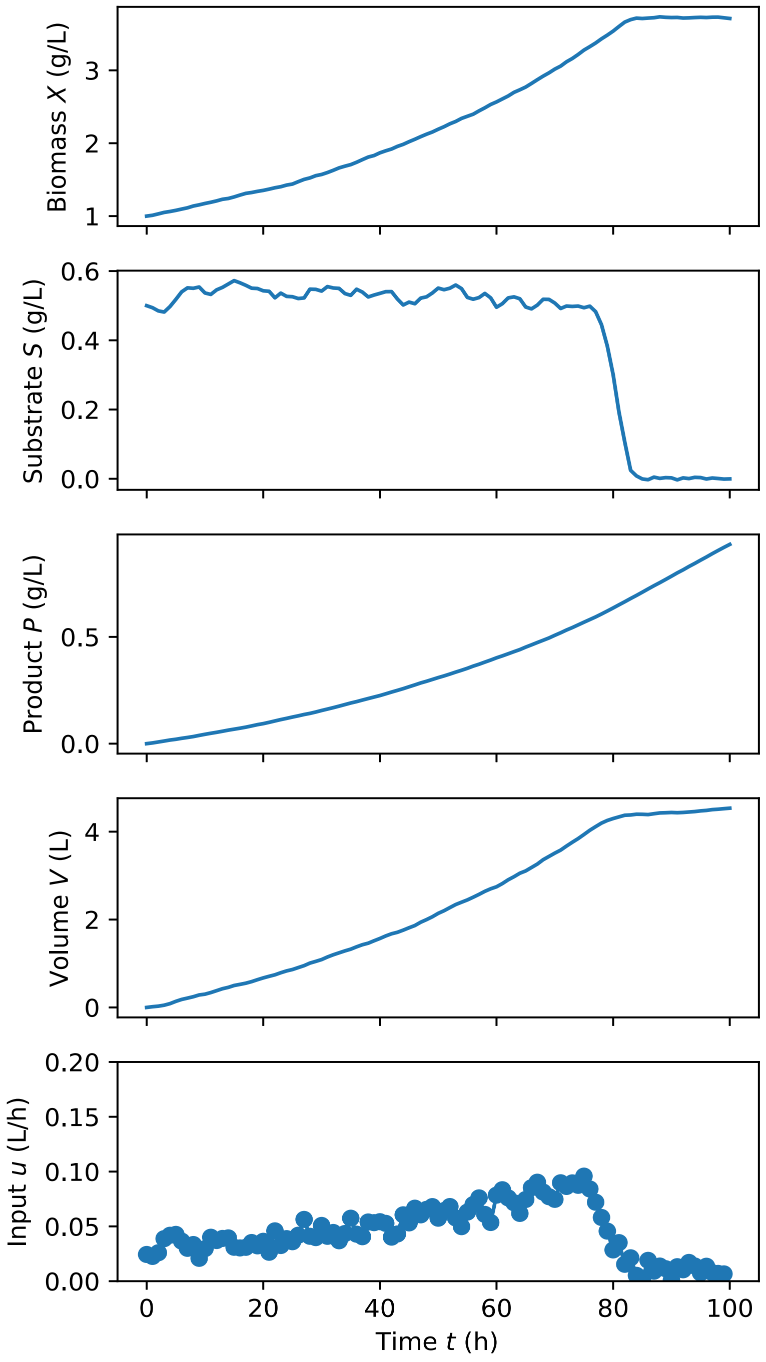

Outline

1. Recap: difference of convex (DC) tube (T)MPC via convex-concave procedure
2. Constructing DC models using polynomial approximations and ICNNs
3. Tube geometry is important!
4. Robustness to disturbances and recursive feasibility
5. Application examples:
   - tiltwing VTOL transition with wind-gust uncertainty
   - robust adaptive control of batch-fed bioreactor
   - data-driven control for closed loop deep brain stimulation

Application: Deep Brain Stimulation (DBS)

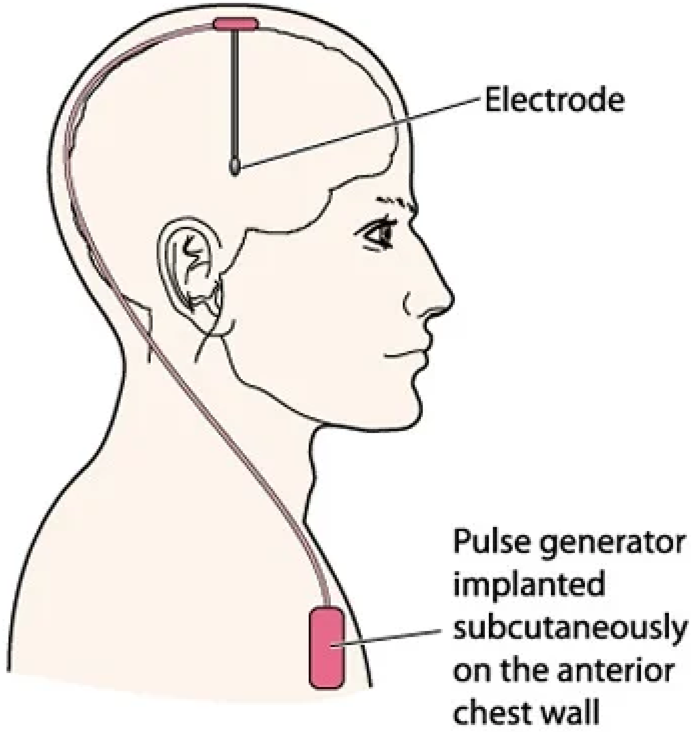

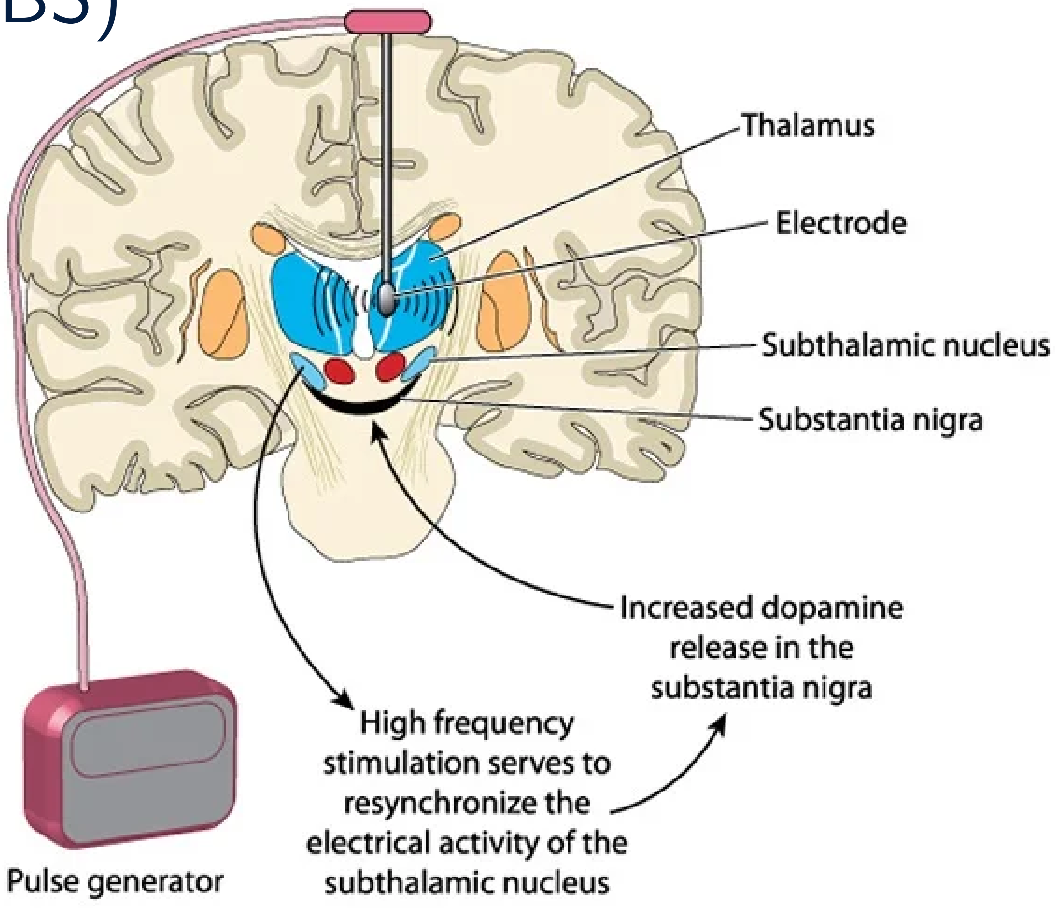

Image Credit: Blamb / Shutterstock.com

DBS treatment for symptoms of Parkinson's disease and essential tremor

Closed loop DBS

Aims:

- Regulate pathological biomarkers (beta oscillations) using feedback from device sensors (implanted electrodes)
- Reduce symptoms with minimal levels of stimulation
- Use aggregated and individual patient data to construct data-driven models

Current status:

- Linear MPC has been validated in simulations
- About to start in vivo testing of linear MPC with online parameter adaptation
- Nonlinear MPC using DC-NNs tested in simulations

Closed loop DBS

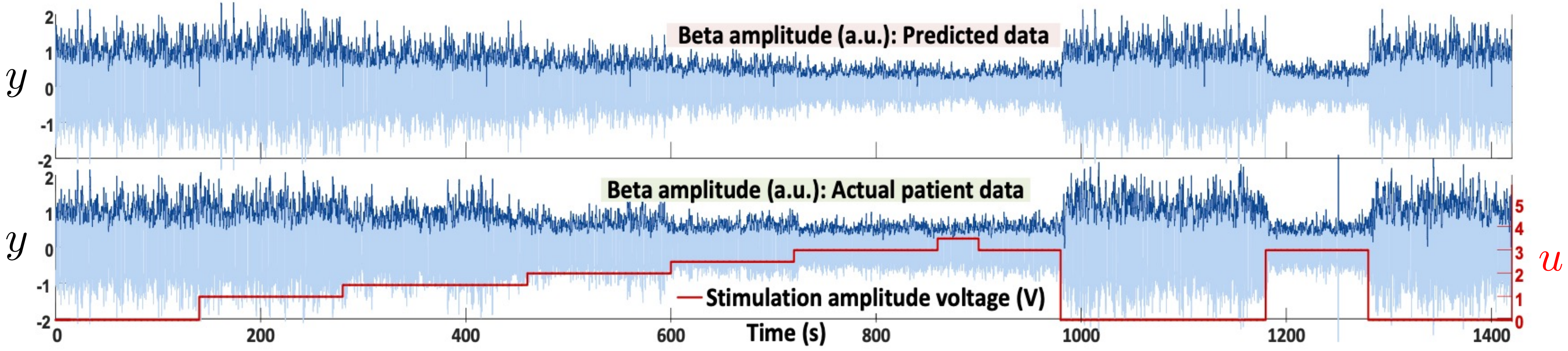

Control problem:

$$\text{minimize} \int_0^T \left(\phi([y(t) - y_0]_+) + Ru(t)^2 \right) dt$$

subject to

$$u \in [0, u_{max}] \quad \dot{u}(t) \in [-\dot{u}_{max}, \dot{u}_{max}]$$

$\phi(\cdot)$: monotonically nondecreasing, $[y - y_0]_+ = \max(y - y_0, 0)$

Closed loop DBS

Discrete-time multistep predictor model:

$$\begin{bmatrix} y_{k+1} \\ y_{k+2} \\ \vdots \\ y_{k+N} \end{bmatrix} = \begin{bmatrix} f_1(x_k, u_k) \\ f_2(x_k, u_{k:k+1}) \\ \vdots \\ f_N(x_k, u_{k:k+N-1}) \end{bmatrix} + \begin{bmatrix} w_1 \\ w_2 \\ \vdots \\ w_N \end{bmatrix}$$

- f_i is a difference of convex functions

$$f_i(x_k, u_{k:k+i-1}) = g_i(x_k, u_{k:k+i-1}) - h_i(x_k, u_{k:k+i-1})$$

$$x_k = (y_{past,k}, u_{past,k})$$

- g_i, h_i are defined by ICNNs trained on observed patient responses
- disturbance bounds are estimated from samples and measurement noise bounds

Multistep DC model for closed loop DBS

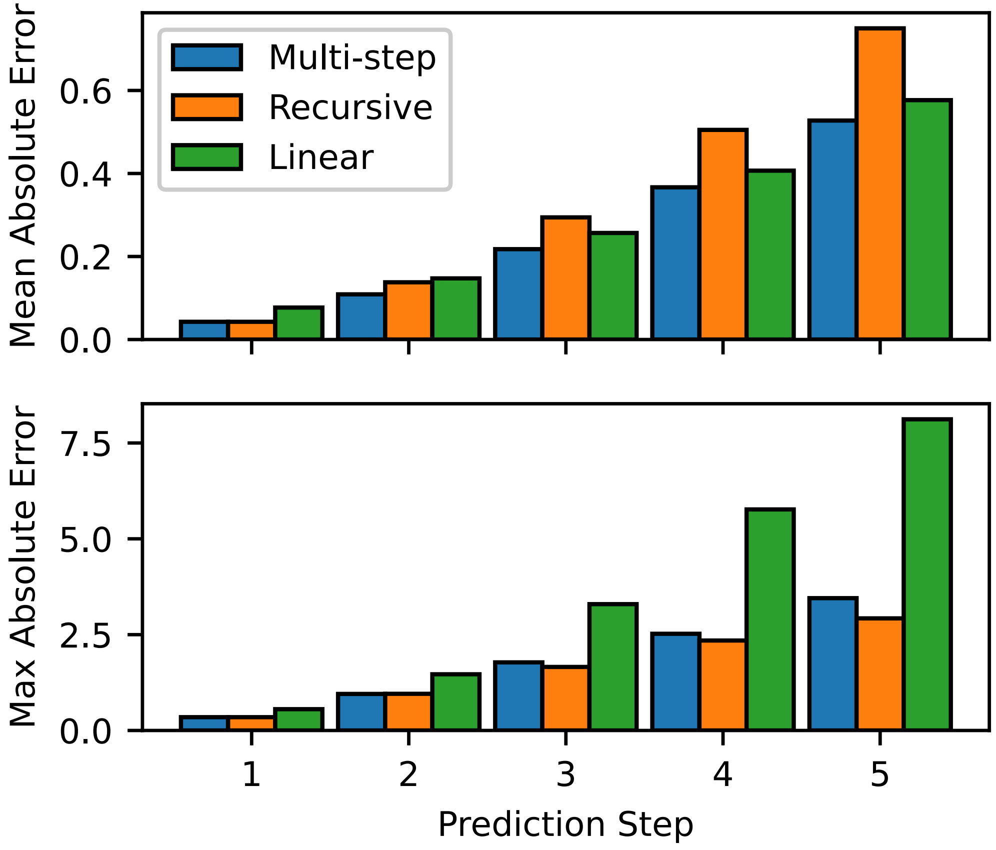

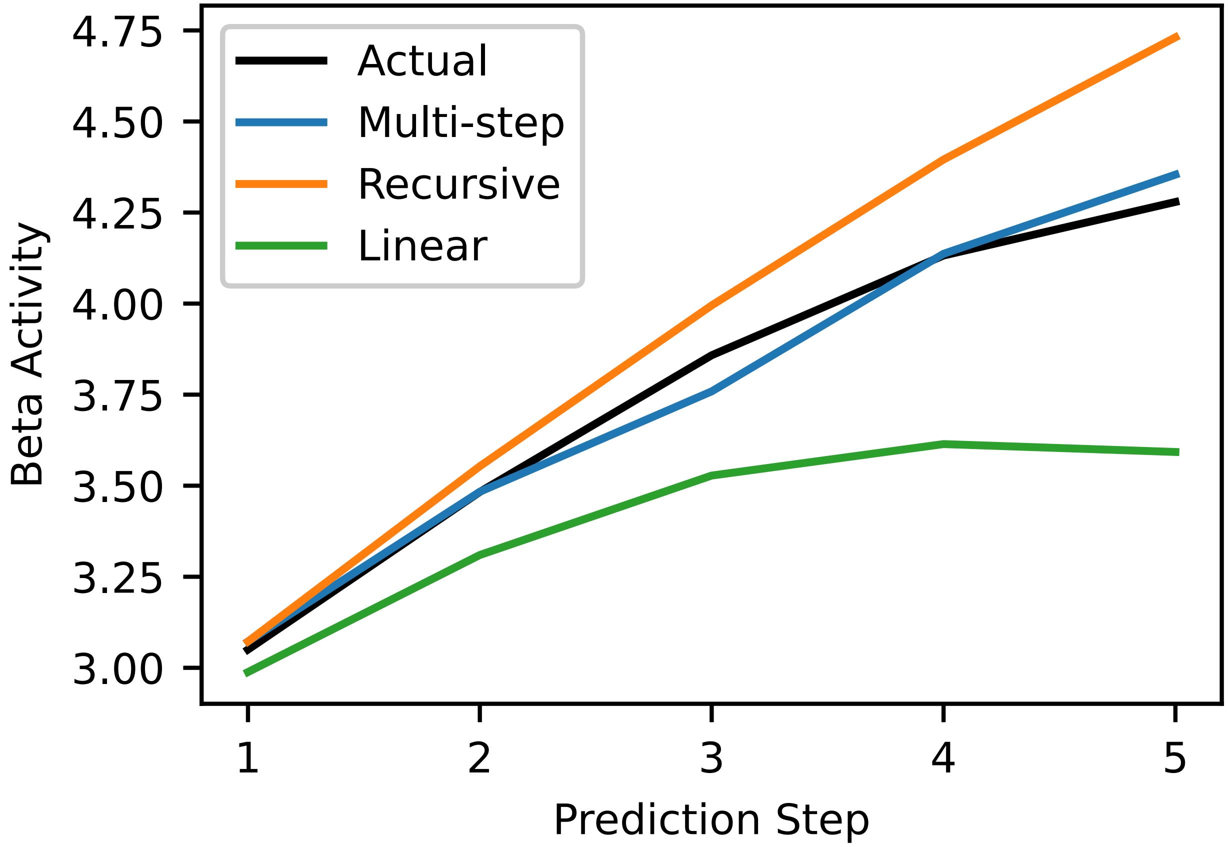

Multi-step predictors outperform linear and nonlinear recursive models

Controller performance

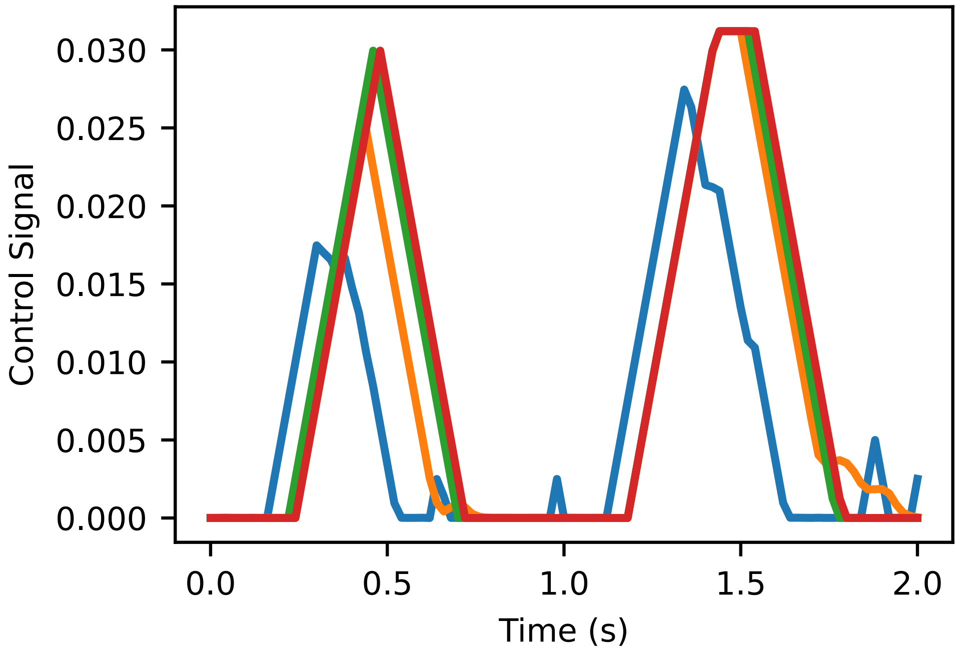

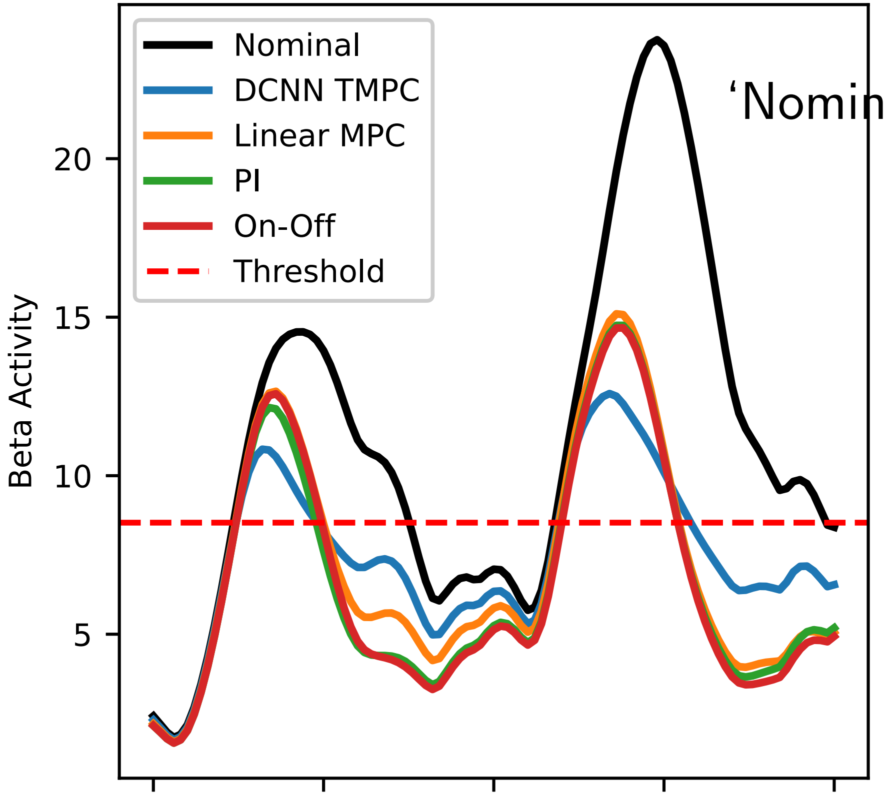

'Nominal' = no control action

- MPC responds faster to bursts of pathological behaviour
- DCNN TMPC provides 30-50% more beta suppression than other controllers
- Stimulation energy 5% less than linear MPC, 20% less than PI & on-off control

Controller performance

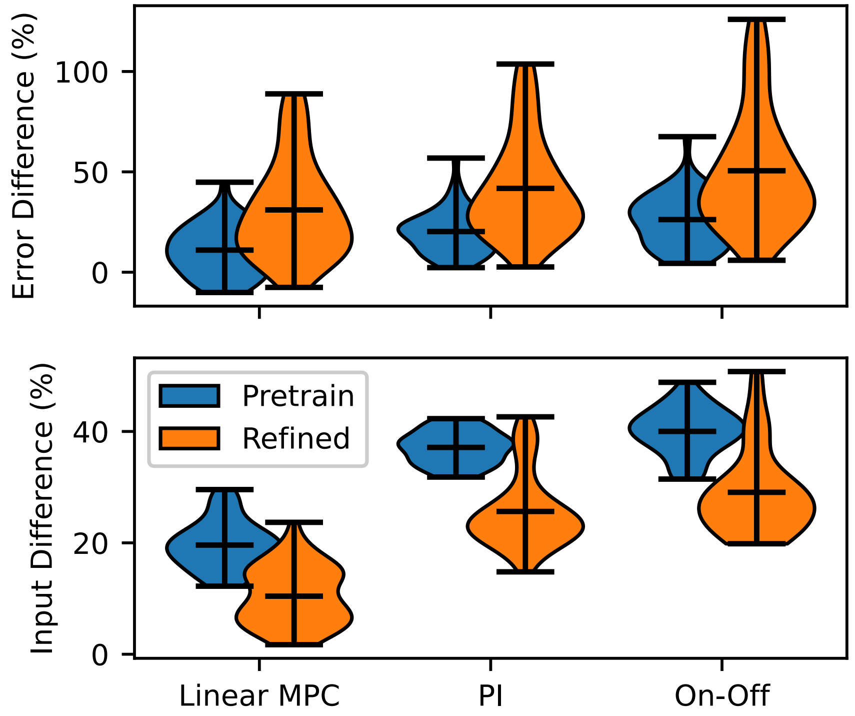

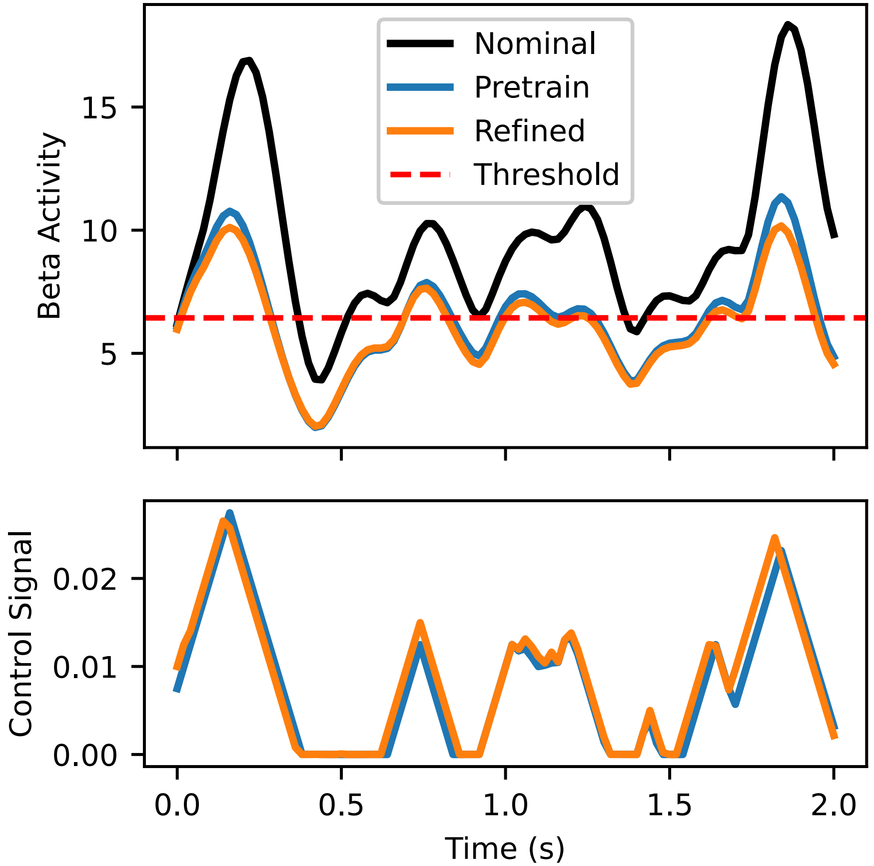

- Pretrained model is derived from LFP data from 3 patients
  Refined model combines this with data from a 4th test patient

- Refined model performs slightly better than pretrained, and significantly better than other controllers

Summary

- DC model representations in MPC:
  - sequential convex programming
  - data-driven DC models using polynomials and DCNNs
- DC-TMPC implementation: model accuracy, computation
  robustness to uncertainty & disturbances
  online parameter estimation
- Ongoing work: dynamics represented as set-valued maps
  applications in aerospace, biomedical, bioprocess control

References

Deep learning adaptive Model Predictive Control of Fed-Batch Cultivations
N. Krausch, M. Doff-Sotta, M. Cannon, P. Neubauer, and M. N. Cruz Bournazou.
Computers & Chemical Engineering (under review) 2025 arXiv:502.01488

A successive convexification approach for robust receding horizon control
Y. Lishkova and M. Cannon.
IEEE Transactions on Automatic Control, 2025 doi:10.1109/TAC.2025.3558253

Deep Learning Model Predictive Control for Deep Brain Stimulation in Parkinson's Disease
S. Steffen and M. Cannon
IEEE *CDC* (under review) 2025 arXiv:2504.00618

Data-driven robust MPC of tiltwing VTOL aircraft
M. Doff-Sotta, M. Cannon, and M. Bacic.
Journal of Guidance, Control, and Dynamics, 2024 doi:10.2514/1.G008315

Safe learning in nonlinear model predictive control
J. Buerger, M. Cannon, and M. Doff-Sotta.
6th L4DC, 2024 proceedings.mlr.press/v242/buerger24a